

RESEARCH ARTICLE

Redefining species concepts for the Pennsylvanian scissor tooth shark, *Edestus*Leif Tapanila^{1,2*}, Jesse Pruitt³

1 Department of Geosciences, Idaho State University, Pocatello, United States of America, **2** Earth Science Division, Idaho Museum of Natural History, Pocatello, United States of America, **3** Idaho Virtualization Lab, Idaho Museum of Natural History, Pocatello, United States of America

* tapaleif@isu.edu

Abstract

This study reevaluates the tooth morphology used to define species within the genus *Edestus* (Chondrichthyes, Euchondrocephali). Known as the scissor tooth shark, *Edestus* produced a unique dentition of spiraled tooth families positioned in the symphysis (midline) of the upper and lower jaws. Morphometric analysis of more than 200 ejected teeth and intact spiral tooth whorls demonstrates that teeth from the upper and lower whorls differ in shape and ontogeny. Comparison of these data to the type specimens of 13 existing species reduces the number of morphologically distinct *Edestus* to just four species and refines the stratigraphic occurrence and expansion of the group. *E. triserratus* has a narrow bullet-shaped crown that points anteriorly and has roots of intermediate length. *E. minor* crowns have a wider triangular base, whereas the crowns of *E. heinrichi* form nearly equilateral triangles and are supported by an elongated root. *E. vorax*, which also has roughly equilateral triangular crowns, has short and deep roots, and is only known from very large specimens that are distinct from the growth series of *E. heinrichi*. Tooth and whorl morphologies among the species are consistent with cranial anatomy observed in a juvenile *E. heinrichi* and with transverse tooth-wear patterns to suggest *Edestus* used a forward to backward slicing motion to bite its prey. Extrapolating body size from tooth whorl length provides a conservative estimate that *E. heinrichi* could exceed 6.7 m in length. *Edestus* fossils are recovered from coastal marine to estuarine deposits spanning roughly six million years (313–307 Ma). *Edestus* first appears in England during the latest Bashkirian (313 Ma, Carboniferous), a few million years after its most closely resembling genus *Lestrodus*. Diversification and range expansion of *Edestus* coincides with the Moscovian transgression that flooded Laurentia and the Russian platform.

OPEN ACCESS

Citation: Tapanila L, Pruitt J (2019) Redefining species concepts for the Pennsylvanian scissor tooth shark, *Edestus*. PLoS ONE 14(9): e0220958. <https://doi.org/10.1371/journal.pone.0220958>

Editor: Giorgio Carnevale, Università degli Studi di Torino, ITALY

Received: June 20, 2019

Accepted: July 26, 2019

Published: September 4, 2019

Peer Review History: PLOS recognizes the benefits of transparency in the peer review process; therefore, we enable the publication of all of the content of peer review and author responses alongside final, published articles. The editorial history of this article is available here: <https://doi.org/10.1371/journal.pone.0220958>

Copyright: © 2019 Tapanila, Pruitt. This is an open access article distributed under the terms of the [Creative Commons Attribution License](https://creativecommons.org/licenses/by/4.0/), which permits unrestricted use, distribution, and reproduction in any medium, provided the original author and source are credited.

Data Availability Statement: All relevant data are within the manuscript and its Supporting Information files.

Funding: This research was partly conducted during sabbatical release time funded by Idaho

Introduction

Chondrichthyans (Euchondrocephali) belonging to the Edestoidea evolved some of the most unusual dental arrangements among vertebrates [1, 2]. The most conspicuous teeth are located in the symphysis of the lower jaw, forming a whorl of sharp, cutting crowns, best exemplified by *Helicoprion* Karpinsky, 1899 [3, 4]. In *Edestus*, both the upper and lower jaws supported symphyseal tooth whorls (whorls, hereafter). Hay [5] first described a specimen showing the

State University. There was no additional external funding received for this study.

Competing interests: The authors have declared that no competing interests exist.

articulated anterior part of *Edestus* having two differently shaped, curved whorls of teeth. Nearly a century later, Zangerl and Jeremiah [6] documented at least three more specimens indicating dimorphism between the upper and lower whorls, but they stopped short of quantifying those differences or placing them in context of the cranium. CT scanning and 2D x-rays of Zangerl and Jeremiah’s specimens confirm a dimorphic upper and lower whorl and reveal their function as opposing cutting surfaces in the mandibular arch [2]. Although much has been gleaned about the form and function of *Edestus* from these specimens, the systematics of *Edestus* remain complicated by the fact that nearly all specimens of *Edestus* whorls lack cranial context or are recovered as individual teeth disaggregated from the whorl.

An *Edestus* whorl is composed of multiple teeth with long V-shaped roots that are stacked *en echelon* like roof tiles (Fig 1). Teeth are generated at the posterior end of the whorl and grow to the anterior end of the whorl, where they are ejected out of the mouth. Teeth are preserved either as single ejected elements, or they are stacked *en echelon* together as part of a whorl containing up to a dozen crowns. According to Zangerl [1] and supported by Tapanila et al. [2], lower whorls generally have a greater curvature than upper whorls, and they both form a spiral that, each, could have produced in excess of 40 teeth during the lifetime of an animal, based on measurements presented here.

As is the case for many chondrichthyans, cranial and post-cranial fossils are uncommon, therefore all 13 species of *Edestus* [7, 8] are defined solely by characters of the tooth crown. Moreover, nearly all species are defined by one specimen, and frequently by one partial crown lacking root material. Taxonomies based on single and incomplete dentitions are vulnerable to narrowly defined species that cannot account for the ontogenetic or environmental variations

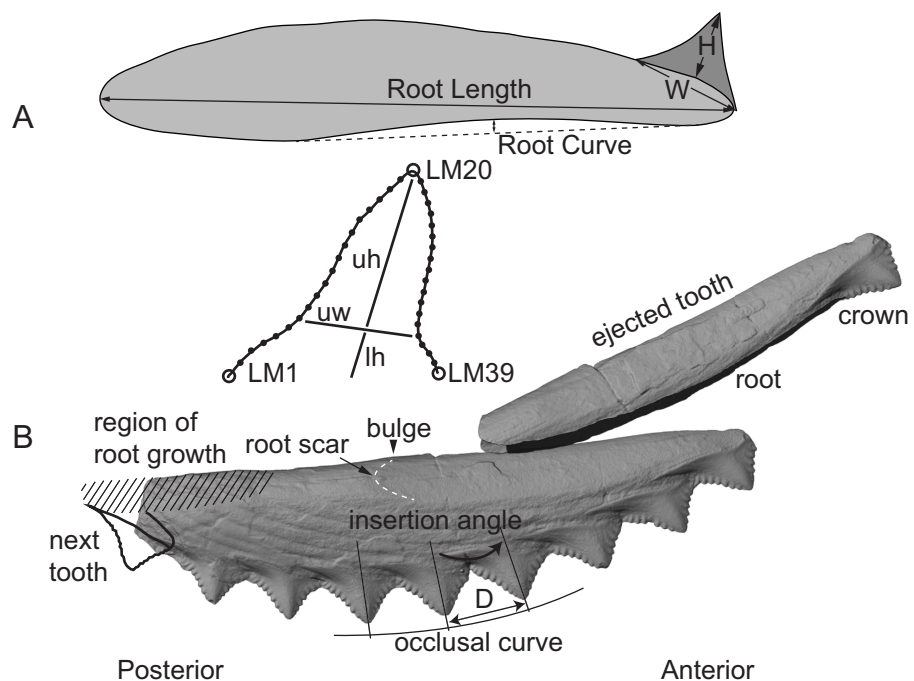


Fig 1. Morphology and terminology of *Edestus* whorl and tooth. (A) Traditional linear measures and geometric landmarks (LM) for individual teeth. (B) Multiple teeth comprise a whorl and are ejected from the anterior end as illustrated. W = crown width; H = crown height; uh = upper height; uw = upper width; lh = lower height; D = distance from crown point to point.

<https://doi.org/10.1371/journal.pone.0220958.g001>

that might affect dental morphology within a species. Such was found to be the case in the edestoid genus *Helicoprion*, where morphometric analysis identified taxobases that resulted in the synonymization of most species founded on single or incomplete specimens [9]. *Edestus* is that much more challenging, considering that *Edestus* teeth are the product of two tooth-families, one from the upper whorl and one from the lower. Once ejected, it is difficult to know if a solitary tooth originated from an upper or lower whorl, and there is no reason to assume both upper and lower teeth have identical shape properties.

Formal revision of *Edestus* taxonomy is well overdue. Although previous reviews on *Edestus* have suggested revised synonymies, they invariably are based on qualitative assessment of few specimens (e.g., [6, 8, 10, 11, 12]). A common observation from most authors is that species concepts for *Edestus* are too narrowly defined, and that most fit within two informally recognized end-members. The “symmetric” group has more equilateral triangular crowns oriented nearly perpendicular to the whorl, whereas the “asymmetric” group has narrow crowns that slant anteriorly. Itano [8] demonstrated that the holotype of *E. minor* had been overlooked for nearly a century and may necessitate revision of several *Edestus* taxa, however, a perceived lack of specimens has thus far hampered any formal attempt (e.g., [7]). Here we aim to rectify the longstanding systematics dilemma by reporting on two extensive collections that provide hundreds of teeth to capture the ontogenetic series and define species concepts for both symmetric and asymmetric *Edestus* groups. This new dataset of measurements is compared against holotypes and referred specimens of established *Edestus* species, and includes specimens known to have associated upper and lower whorls (Table 1). Taxonomic revision provides a clearer history on the range expansion and jaw morphologies of the unusual scissor tooth shark.

Table 1. Type specimens and figure references for previously defined *Edestus* species considered in this study.

Crown shape	Revised species	specimen number	Types and Previous designation	Image reference
Symmetric	<i>E. heinrichi</i>	USNM V 182450	Holotype <i>E. crenulatus</i>	This study, Fig 2K
	<i>E. heinrichi</i>	n/a	Illustration of holotype <i>E. heinrichi</i>	Newberry and Worthen, 1870 [13], pp. 350–353, pl. 1, Fig 1
	<i>E. heinrichi</i>	PIN RAN 1988/2	Holotype <i>E. karpinskyi</i>	Lebedev, 2001 [14], Pl. 44, Fig 7B
	<i>E. heinrichi</i>	n/a	Holotype <i>E. protopirata</i>	Trautschold, 1879 [15], Pl. VI, Fig 8A
	<i>E. heinrichi</i>	USNM 6049	Holotype <i>E. serratus</i>	This study, Fig 2L
	<i>E. vorax</i>	AMNH 225	Holotype <i>E. giganteus</i>	This study, Fig 2O
Asymmetric	<i>E. vorax</i>	ANSP 9899	Holotype <i>E. vorax</i>	Leidy, 1856 [16], Fig 3A
	<i>E. minor</i>	AMNH FF477	Holotype, broken <i>E. minor</i>	Itano, 2014 [8], Fig 10
	<i>E. minor</i>	USNM 7255	Holotype <i>E. mirus</i>	This study, Fig 2F
	<i>E. minor</i>	GSM 49368	Type <i>E. pringlei</i>	This study, Fig 2C
	<i>E. triserratus</i>	GSM 31410	Holotype <i>E. triserratus</i>	This study, Fig 2E
	<i>E. triserratus</i>	PIN RAN 2804/726	Holotype <i>E. kolomensis</i>	Lebedev, 2001 [14], Pl. 44, Fig 5
	<i>E. triserratus</i>	TSNiGR 11/1865	Holotype <i>E. minusculus</i>	Karpinsky, 1899 [3], Pl. IV, Fig 13

<https://doi.org/10.1371/journal.pone.0220958.t001>

Material and methods

The two primary collections of *Edestus* used in this study were assembled by Zangerl (FMNH) and Jeremiah (ANSP). The Zangerl collection includes dozens of specimens recovered from shale quarries of the Staunton and Linton formations in Illinois. Zangerl and Richardson [17] detail the excavation and description of the Mecca and Lloyd quarries, wherein hundreds of fish fossil were recovered from shallow marine transgressive deposits of Desmoinesian age (Late Carboniferous, Pennsylvanian). Most specimens are single teeth, and also include several intact whorls. Specimens embedded in shale matrix were imaged with x-ray digital photography. Results generated from x-ray and photographic images yield overlapping measurements, validating the use of these two methods. Rare examples of associated cranial material (e.g., [6]) were examined to identify upper and lower whorl morphology in context of the jaw. Both asymmetric and symmetric teeth are present in the collection.

The Jeremiah collection includes half a dozen whorls and more than 40 specimens of complete or broken individual teeth. Although the specimens were collected without geological description, we have unpublished correspondence from Zangerl (pers. comm., 2003) indicating they were recovered from collapsed shale rocks that formed the roofs of abandoned coal mines. Presumably, these shales record marine or estuarine flooding deposits above coal marshes, similar to the fossils from the Zangerl collection. All specimens are from the Carbonale Formation in Illinois and are Desmoinesian in age (Late Carboniferous, Pennsylvanian). Only symmetric-crowned teeth comprise the Jeremiah collection.

In addition to these two collections, type and referred specimens of *Edestus* species were analyzed, giving our measured dataset a total of 141 specimens that include 212 measured tooth crowns. Updated stratigraphic and geographic summaries of *Edestus* add to previous summaries [12, 18], and use regional correlations to present occurrences in the global Pennsylvanian time scale [19].

Morphological analysis of *Edestus* followed traditional measurement and geometric approaches. Linear dimensions and ratios summarized in Fig 1 were measured from photographs, x-rays, or directly from specimens. *Edestus* specimens were first grouped based on asymmetric versus symmetric crown shape. Measurements and ratios are summarized by mean values and their relationships evaluated using ordinary least squares on log-log transformed values assuming allometric growth. Taxobases found to be helpful in describing the edestoid, *Helicoprion* [9] were assessed for their utility in defining *Edestus* species. Curvature of the whorl was assessed by measuring the angle between crowns (e.g., insertion angle: [9]) and distance between crown tips (D). The angle between two crowns is estimated by drawing lines that bisect each crown, and measuring the acute angle between them. Plotting cumulative distance and angle gives an estimated radius of curvature for the occlusal curve of the whorl. Sixteen whorls with intact series of crowns are presented, including holotypes for *E. mirus*, *E. crenulatus*, *E. serratus*, and *E. heinrichi*. The holotype of *E. mirus* and the specimen FMNH PF8047 are unique in providing both upper and lower whorls in association.

Geometric morphometrics was used to examine crown shape in 99 specimens of *Edestus*. Using tpsDig v. 2.16, three type 2 landmarks (LM1, LM20, LM39) were identified on the crown and these were connected with two series of equidistant semilandmarks to approximate the shape of the cutting surface (39 points total). Crown shapes were rotated and scaled using a full Procrustes superposition prior to generating covariance matrices and principle components analysis in MorphoJ v.1.05c. Results of the PCA identify shape parameters of the crown that might reveal one or more ontogenetic series that provides a partial basis for species discrimination. PC scores are then related to traditional measurement data such that species concepts are defined by linear measures more readily useful for diagnosing specimens.

All type specimens are included in the geometric analysis except the holotypes of *E. vorax* (ANSP 9899) and *E. triserratus* (GSM31410), which lack the crown apex, landmark 20. These specimens are included later in the methodology by approximating the geometric ordination using linear measurements and ratios. Recommendation for synonymy follows International Code of Zoological Nomenclature Article 23 giving priority to senior synonyms [20].

Nomenclatural acts

The electronic edition of this article conforms to the requirements of the amended International Code of Zoological Nomenclature, and hence the new names contained herein are available under that Code from the electronic edition of this article. This published work and the nomenclatural acts it contains have been registered in ZooBank, the online registration system for the ICZN. The ZooBankLSIDs (Life Science Identifiers) can be resolved and the associated information viewed through any standard web browser by appending the LSID to the prefix "<http://zoobank.org/>". The LSID for this publication is: urn:lsid:zoobank.org:pub:A83F549C-150F-4A8A-9B40-298EBF07B00B. The electronic edition of this work was published in a journal with an ISSN, and has been archived and is available from the following digital repositories: PubMed Central, LOCKSS.

Institutional abbreviations for specimens

ACM, Beneski Museum of Natural History, Amherst College, Amherst, U.S.A.; **AMNH**, American Museum of Natural History, New York, U.S.A.; **ANSP**, Academy of Natural Sciences Museum, Philadelphia, U.S.A.; **CAS**, Chicago Academy of Science, Chicago, U.S.A.; **DMNH**, Denver Museum of Nature and Science, Denver, U.S.A.; **FMNH**, Field Museum of Natural History, Chicago, U.S.A.; **GSM**, British Geological Survey, Keyworth, Great Britain; **ISM**, Illinois State Museum, Springfield, U.S.A.; **KGS**, Kentucky Geological Survey, Lexington, U.S.A.; **PIN**, Palaeontological Institute of the Russian Academy of Sciences, Moscow, Russia; **TMM**, Vertebrate Paleontology Laboratory, University of Texas, Austin, U.S.A.; **TSNiGR**, Central Research Geological Museum, St.-Petersburg, Russia; **USNM**, National Museum of Natural History, U.S.A.

Results

Morphometry and establishment of taxobases

Description and measures of the whorl. *Edestus* whorls all share several traits. The cutting (occlusal) surface forms a convex series of serrated crowns. Crown size decreases anteriorly, but in many specimens teeth within a single whorl are nearly the same size. Tooth roots are incrementally longer from posterior to anterior position along the whorl. The anteriormost two or three teeth in the series all have equal root length. This suggests that growth of the root occurs in a relatively small region at the posterior end of the whorl (Fig 1B). The base of the whorl either has an outline that is shallowly or deeply concave. The base is interrupted by a subtle convexity (bulge) located halfway along the whorl; its position is further anterior in whorls with teeth having shorter roots. Anterior to the bulge is a scar marking the attachment point of the most recently ejected tooth. In associated specimens, the lower whorl displays greater curvature, especially in the concave base of the whorl, whereas the upper whorl has a comparatively straighter base. Whorls with symmetric teeth include the largest specimens of *Edestus* (e.g., holotype of *E. giganteus*, AMNH 225), and include concave and straight-based whorls. Straight-based whorls are less common in the asymmetric-toothed group; only two specimens are known in this study (Jillson and CAS), whereas all others have broadly concave whorls.

Geometry of the whorl is quantified in two ways, the insertion angle and occlusal curvature (Figs 1B and 4). Insertion angle varies greatly among pairs of *Edestus* crowns, from 2° to 22°, and is sensitive to specimen size. An individual whorl may include ~5–12 crowns, and represents a relatively short ontogenetic series for the animal. Within a single whorl, insertion angle does not vary much, and small deviations may be attributed to measurement error. Only the Jilison ([21], S1 Fig) specimen shows a significant flattening of curvature along the base of the whorl that cannot be accounted for by taphonomic effects.

Summing the insertion angle between crowns over the length of a whorl (starting from the anterior, more juvenile teeth) gives a cumulative curvature of the occlusal surface. *Edestus* whorls in this study have occlusal curves that range in radius between 5 and 45 cm. Generally, as crown width (W) increases, spacing between crown apices (D) increases, and so does insertion angle. It follows that juvenile whorls are more tightly curved than their adult counterparts. Further, our limited dataset suggests that asymmetric-crowned whorls maintain higher curvature at large size compared to symmetric-crowned whorls (e.g., FMNH PF 2317 versus ANSP 22393). The holotype *E. giganteus* (AMNH 225) is an outlier in having the largest teeth and the most gently curved whorl (45 cm radius) of any specimen.

Given that occlusal curvature varies with size, a growth series could be ascertained. Unfortunately, the small number of complete whorls makes insertion angle and its aggregate, the occlusal curve, unlikely to be useful quantitative taxobases to distinguish *Edestus* species at this time.

Linear measures of teeth. Crown and root proportions of *Edestus* teeth distinguish symmetric versus asymmetric specimens (Tables 2 and 3). Specifically, the height to width ratio (H:W) of the tooth crown (Fig 5) shows distinct populations for each basic form. Asymmetric crowns are the tallest of the two forms with a mean H:W of 1.08. Log-log transformed height versus width has a strong linear relationship ($r^2 = 0.87$, $p = 0.0001$). The ratio of root length to crown width has a mean of 3.8 for the asymmetric group, and has a strong linear relationship when log-log transformed ($r^2 = 0.87$, $p < 0.0001$). Variation in root proportions for a given tooth size can be attributed to incomplete growth in the root. For both ratios, the asymmetric crowns of the holotype *E. triserratus*, *E. mirus*, *E. pringlei*, *E. minusculus*, *E. minor*, and *E. kolomnensis* fit closely within the population of FMNH specimens.

Teeth within a whorl are measured separately and their position in the whorl is annotated in the specimen identifier with a sequential decimal suffix (e.g., .1 is the anterior-most tooth, .2 is the adjacent tooth to the posterior, etc.). Type = Original species diagnoses: hein = *E. heinrichi*; cren = *E. crenulatus*; serr = *E. serratus*; karp = *E. karpinskyi*; proto = *E. protopirata*; vorax = *E. vorax*; gigan = *E. giganteus*. Elem. = Element: t = tooth; w = whorl. Posn = Position: l = lower whorl; u = upper whorl. All tooth measurements presented in cm, and defined in Fig 1.

The population of all symmetric crowns, composed mostly of ANSP and FMNH teeth, have a mean H:W of 0.61, much lower than the asymmetric group. Log-log transformed height versus width has a strong linear relationship ($r^2 = 0.81$, $p = 0.0001$). The high variance of H:W is observed even among multiple crowns from the same whorl. For example, 12 crowns measured from ANSP 22393 have H:W ranging between 0.55 and 0.70. The holotypes of *E. crenulatus*, *E. heinrichi*, *E. protopirata*, *E. serratus*, *E. karpinskyi* plot at or slightly above the mean with H:W consistently < 0.80 , whereas the very large crowns of the holotypes *E. vorax* and *E. giganteus* plot closer to the asymmetric group mean with H:W > 0.9 .

The roots of symmetric-crowned teeth are proportionately longer than the asymmetric group, with a mean root-length to width ratio of 4.9, and their log-log transformed values have a strong linear relationship ($r^2 = 0.87$, $p < 0.0001$). This value increases to 6 with the largest teeth (3 cm width). Again, *E. vorax* and *E. giganteus* are the only holotypes with symmetric crowns that plot as outliers, having short roots only 2.5 to 4 times greater than crown width.

Table 2. Tooth metrics for *Edestus* specimens.

Specimen		Elem.	Posn.	Type	Crown W	Crown H	H:W	Root L
<i>Edestus heinrichi</i>								
ANSP	22376	t			3.13	1.75	0.56	18.46
ANSP	22378	t			2.35	1.24	0.53	
ANSP	22379	t			3.71	2.29	0.62	
ANSP	22380	t			2.12	1.75	0.83	
ANSP	22381	t			2.60	1.48	0.57	
ANSP	22382	t			3.13	1.35	0.43	
ANSP	22383	t			3.08	1.23	0.40	
ANSP	22384	t			3.59	1.86	0.52	
ANSP	22387	t			2.18	1.15	0.53	
ANSP	22390	t			3.20	1.88	0.59	
ANSP	22398	t			2.61	1.68	0.64	
ANSP	22399	t			3.67	1.74	0.47	
ANSP	22400	t			3.98	1.75	0.44	
ANSP	22401	t			3.34	1.61	0.48	
ANSP	22402	t			2.42	1.49	0.61	
ANSP	22403	t			3.02	1.67	0.55	
ANSP	22404	t			3.12	1.50	0.48	
ANSP	22405	t			2.39	1.28	0.54	
ANSP	22406	t			1.21	0.94	0.77	
ANSP	22412	t			2.40	1.46	0.61	10.45
ANSP	22413	t			1.97	1.07	0.54	9.40
ANSP	22414	t			2.79	1.28	0.46	
ANSP	22415	t			1.79	1.12	0.63	
ANSP	22416	t			3.25	1.59	0.49	
ANSP	22417	t			3.75	1.88	0.50	
ANSP	22418	t			2.38	1.35	0.57	
ANSP	22419	t			3.68	1.53	0.42	
ANSP	22420	t			1.77	0.93	0.53	
ANSP	22423	t			3.14	1.41	0.45	
ANSP	22424	t			2.81	1.26	0.45	
ANSP	22425	t			1.27	0.63	0.50	
ANSP	22426	t			1.65	1.57	0.95	
ANSP	22428	t			2.48	1.76	0.71	
ANSP	22430	t			2.73	1.66	0.61	
ANSP	22431	t			2.28	0.88	0.39	
ANSP	22433	t			3.09	1.96	0.63	
ANSP	22435	t			2.15	0.86	0.40	
ANSP	22436	t			2.56	1.20	0.47	
FMNH	Barret #6	t			0.92	0.78	0.84	7.63
FMNH	C67 Dr 15-4	t			1.74	0.91	0.52	8.19
FMNH	CompPenn#17	t						8.61
FMNH	HQ114	t			1.51	1.11	0.74	
FMNH	HQ1329 B-1	t			2.62	1.78	0.68	13.11
FMNH	HQ1344-B-2	t			2.62	1.46	0.56	11.57
FMNH	HQ46	t			1.53	1.10	0.72	10.81
FMNH	HQ554 A-2	t			1.04	0.59	0.57	4.89

(Continued)

Table 2. (Continued)

Specimen	Elem.	Posn.	Type	Crown W	Crown H	H:W	Root L
FMNH	HQ555 B-1	t		1.15	0.72	0.63	6.44
FMNH	HQ610 A-3	t		1.27	0.78	0.61	7.00
FMNH	HQ66	t		2.41	0.97	0.41	
FMNH	HQ69,70(B)	t		0.64	0.28	0.43	3.42
FMNH	HQ799 B-1	t		2.77	1.36	0.49	
FMNH	HQ983 A-2	t		1.54	0.83	0.54	6.07
FMNH	Jelliff#2	t		3.02	1.49	0.49	
FMNH	L238	t		1.70	0.78	0.46	8.06
FMNH	L250	t		2.12	1.19	0.56	8.50
FMNH	L309 (J864)	t		1.68	0.85	0.51	7.98
FMNH	L310 (J629)	t		0.59	0.44	0.76	2.99
FMNH	L310 (J859)	t		0.37	0.27	0.73	1.75
FMNH	L311 (J1068)	t		2.57	1.42	0.55	11.26
FMNH	L311 (J288)	t		1.65	0.93	0.56	6.91
FMNH	L311 (J938)	t		1.93	1.01	0.52	8.01
FMNH	L312(J61)	t		1.54	1.00	0.65	7.20
FMNH	L314	t		1.75	1.25	0.71	7.97
FMNH	L315A(PF2320)	t		2.28	1.28	0.56	10.11
FMNH	L316	t		2.38	1.66	0.70	
FMNH	L317(2314)	t		0.55	0.60	1.09	4.31
FMNH	Logan 115 (J657)	t		1.14	0.96	0.84	6.25
FMNH	MontgomeryCk dr5	t		2.04	1.30	0.64	9.15
FMNH	MQ236 (PF2852)	t		1.98	1.65	0.84	
FMNH	PF2320	t		2.40	1.56	0.65	10.22
FMNH	PF-2323	t		1.60	0.93	0.58	7.27
FMNH	PF-2330	t		0.53	0.32	0.61	1.82
FMNH	PF2331 J-122	t		2.32	1.44	0.62	6.98
FMNH	PF2335 J288	t		2.01	1.10	0.55	6.83
FMNH	PF-2339	t		1.16	0.69	0.60	
FMNH	PF-2341	t		0.63	0.49	0.79	2.38
FMNH	PF-8049	t		2.12	1.62	0.76	
FMNH	PF-8404	t		3.14	1.60	0.51	
FMNH	Pit 14(17&18)	t		2.45	1.03	0.42	
FMNH	Pit 14(Peabody Coal)	t		2.27	1.11	0.49	
FMNH	Q208	t		1.26	0.76	0.60	6.39
FMNH	UC3316	t		3.02	1.47	0.49	
ANSP	22377	t	l	2.71	1.38	0.51	17.39
ANSP	22411	t	l	2.97	1.16	0.39	11.67
FMNH	C67 Dr 15-1	t	l	2.18	0.98	0.45	13.05
FMNH	C67 Dr 15-3	t	l	2.33	1.11	0.47	13.07
FMNH	CompPenn#19	t	l	1.63	1.00	0.61	11.70
FMNH	Fish pit 12	t	l	1.67	0.95	0.57	11.79
FMNH	HQ1374 A-3	t	l	2.31	1.26	0.55	14.27
FMNH	PF-1024	t	l	2.00	1.02	0.51	10.56
FMNH	X-Ray #10	t	l	2.01	0.89	0.44	11.21
ANSP	22391 .1	w	u	2.33	1.61	0.69	12.39
ANSP	22391 .2	w	u	2.34	1.55	0.66	12.33

(Continued)

Table 2. (Continued)

Specimen	Elem.	Posn.	Type	Crown W	Crown H	H:W	Root L	
ANSP	22391 .3	w	u		2.23	1.67	0.75	
ANSP	22391 .4	w	u		2.22	1.63	0.73	
ANSP	22391 .5	w	u		2.08	1.63	0.79	
ANSP	22391 .6	w	u		2.27	1.69	0.74	
ANSP	22392 J-3 .1	w	u		3.23	1.89	0.58	17.58
ANSP	22392 J-3 .2	w	u		3.25	1.96	0.60	17.35
ANSP	22392 J-3 .3	w	u		3.04	1.81	0.60	15.84
ANSP	22392 J-3 .4	w	u		3.14	1.87	0.60	14.37
ANSP	22392 J-3 .5	w	u		2.88	1.79	0.62	12.52
ANSP	22392 J-3 .6	w	u		3.03	1.95	0.64	
ANSP	22392 J-3 .7	w	u		2.86	1.75	0.61	
ANSP	22392 J-3 .8	w	u		2.69	1.71	0.64	
ANSP	22396 J-1 .1	w	u		3.01	1.51	0.50	19.41
ANSP	22396 J-1 .2	w	u		3.08	1.76	0.57	19.37
ANSP	22396 J-1 .3	w	u		2.82	1.61	0.57	19.40
ANSP	22396 J-1 .4	w	u		3.26	1.77	0.54	19.50
ANSP	22396 J-1 .5	w	u		3.10	1.76	0.57	
ANSP	22396 J-1 .6	w	u		3.03	1.83	0.60	
ANSP	22396 J-1 .7	w	u		3.05	1.81	0.59	
ANSP	22396 J-1 .8	w	u		2.80	1.86	0.66	
ANSP	22396 J-1 .9	w	u		2.87	1.79	0.62	
ANSP	22396 J-1 .10	w	u		2.64	1.78	0.68	
ANSP	22396 J-1 .11	w	u		2.62			
FMNH	PF-2845	w	u		0.44	0.37	0.84	
FMNH	PF-8735 .1	w	u					20.20
FMNH	PF-8735 .2	w	u		3.50	2.00	0.57	19.20
FMNH	PF-8735 .3	w	u		3.30	1.80	0.55	19.00
FMNH	PF-8735 .4	w	u		3.40	2.00	0.59	17.70
FMNH	PF-8735 .5	w	u		3.30	1.90	0.58	15.70
FMNH	PF-8735 .6	w	u		3.30	2.00	0.61	
FMNH	PF-8735 .7	w	u		3.40			
FMNH	PF-8735 .8	w	u		3.20	2.10	0.66	
FMNH	PF-8735 .9	w	u		3.20			
FMNH	UF30 .1	w	u		3.10	1.80	0.58	16.90
FMNH	UF30 .2	w	u		3.00			16.60
FMNH	UF30 .3	w	u		3.00			16.50
FMNH	UF30 .4	w	u		3.00			15.80
FMNH	UF30 .5	w	u		2.90			14.50
FMNH	UF30 .6	w	u		2.90			
FMNH	UF30 .7	w	u		2.90			
FMNH	UF30 .8	w	u		2.80	2.10	0.75	
FMNH	UF30 .9	w	u		2.80	2.10	0.75	
FMNH	HeslerQ 26	w	l		1.52	0.81	0.53	7.13
ANSP	22373 J-5 .1	w	l		3.25	1.73	0.53	21.65
ANSP	22373 J-5 .2	w	l		3.48	1.68	0.48	21.33
ANSP	22393 J-4 .1	w	l		3.28	1.84	0.56	22.09
ANSP	22393 J-4 .2	w	l		3.29	1.83	0.56	

(Continued)

Table 2. (Continued)

Specimen		Elem.	Posn.	Type	Crown W	Crown H	H:W	Root L
ANSP	22393 J-4 .3	w	l		3.21	1.80	0.56	
ANSP	22393 J-4 .4	w	l		3.38	1.86	0.55	
ANSP	22393 J-4 .5	w	l		3.31	1.91	0.58	
ANSP	22393 J-4 .6	w	l		3.41	1.91	0.56	
ANSP	22393 J-4 .7	w	l		3.07	2.04	0.66	
ANSP	22393 J-4 .8	w	l		3.20	1.95	0.61	
ANSP	22393 J-4 .9	w	l		3.25	2.27	0.70	
ANSP	22393 J-4 .10	w	l		3.11	1.84	0.59	
ANSP	22393 J-4 .11	w	l		3.00	2.11	0.70	
ANSP	22393 J-4 .12	w	l		3.14	1.84	0.59	
PIN	RAN 1988/1	t			2.87	2.30	0.80	13.78
AMNH	488 cast	w	u		2.98	2.03	0.68	16.55
n/a	Newberry and Worthen, 1870 [13],	w	u	hein	2.98	2.08	0.70	16.50
USNM	V 182450 .1	w	u	cren	3.18			16.48
USNM	V 182450 .2	w	u	cren	2.80			15.73
USNM	V 182450 .3	w	u	cren	2.84	1.64	0.58	14.80
USNM	V 182450 .4	w	u	cren	2.70	1.74	0.64	13.71
USNM	V 182450 .5	w	u	cren	2.85			
USNM	V 182450 .6	w	u	cren	2.58	1.58	0.61	
USNM	6049 .2	w	u	serr	2.62	1.93	0.73	12.18
USNM	6049 .3	w	u	serr	2.46	2.00	0.81	11.40
USNM	6049 .4	w	u	serr	2.46	1.92	0.78	9.71
USNM	6049 .5	w	u	serr	2.29	1.86	0.81	
USNM	6049 .6	w	u	serr	2.25			
PIN	RAN 1988/2	t		karp	2.90	2.15	0.74	14.00
n/a	Trautschold [15]	t		proto	3.00	2.20		
<i>Edestus vorax</i>								
ANSP	9899	w		vorax	4.46	4.16	0.93	11.97
AMNH	225	w		gigan	6.85	8.36	1.22	29.15
KGS	Greb et al. 2011 [22]	w			4.76	4.03	0.85	21.65

<https://doi.org/10.1371/journal.pone.0220958.t002>

Geometric morphometrics of tooth crowns. Geometric analysis of all *Edestus* tooth crowns demonstrates distinct populations for the asymmetric and symmetric specimens (Fig 6). The first principle component captures 88% of crown shape variation, with positive values corresponding to a short, stout, and symmetrical crown. The holotypes of *E. protopirata*, *E. crenulatus*, *E. heinrichi*, *E. serratus*, *E. karpinskyi*, and *E. giganteus* fit in this grouping of positive PC1 space. In negative PC1 space, the apex is deflected anteriorly, and the overall crown is narrow and tall. The asymmetric-crowned holotypes of *E. kolomnensis*, *E. pringlei*, *E. minusculus*, *E. mirus* (both upper and lower whorl teeth) and *E. minor* fit in this population. Given the distinct populations from the analysis of all specimens, the symmetric and asymmetric groups were each analyzed separately.

Principle components analysis of the symmetric group results in a similar distribution of shape observed in the combined analysis (Fig 7A and S1 Appendix). Positive PC1 corresponds to a short, wide crown typified by the holotypes of *E. heinrichi* and *E. crenulata*, whereas the holotypes of *E. protopirata*, *E. karpinskyi*, and *E. serratus* occupy negative PC1 space. The holotype of *E. giganteus* is an outlier in negative PC1 space, with a very tall crown. Positive PC2

Table 3. Tooth metrics for asymmetric-crowned *Edestus* specimens.

Specimen		Elem	Posn	Type	Crown W	Crown H	Crown H:W	Crown uw	Crown uh	Crown uw:uh	Crown lh	Root L
<i>Edestus minor</i>												
AMNH	FF 477	t		minor	1.83	2.51	1.37	1.22	1.58	0.77	0.93	
USNM	7255 .2 low	w	l	mirus	2.24	2.47	1.10	1.35	1.63	0.83	0.84	
USNM	7255 .3 low	w	l	mirus	2.03	2.55	1.26	1.40	1.77	0.79	0.78	
USNM	7255 .4 low	w	l	mirus	2.00	2.57	1.29	1.59	1.83	0.87	0.74	
USNM	7255 .5 low	w	l	mirus	2.20	2.67	1.21	1.40	1.62	0.86	1.05	
USNM	7255 .2 up	w	u	mirus	2.59	2.45	0.95	1.63	1.82	0.90	0.63	
USNM	7255 .3 up	w	u	mirus	2.61	2.74	1.05	1.66	2.02	0.82	0.72	10.00
USNM	7255 .4 up	w	u	mirus	2.71	2.54	0.94	1.71	1.81	0.94	0.73	
USNM	7255 .5 up	w	u	mirus	2.68	2.92	1.09	1.80	2.05	0.88	0.87	
GSM	49368	t		pring	1.26	1.56	1.24	0.90	1.18	0.76	0.38	3.89
TMM	40234–8	t			2.83	2.60	0.92	1.53	1.58	0.97	1.02	
FMNH	HQ42	t			1.97	1.68	0.85	1.42	1.61	0.88	0.07	5.71
FMNH	HQ435 B4	t			2.63	2.57	0.98	1.54	1.96	0.79	0.61	
FMNH	HQ65	t			0.73	0.80	1.10	0.51	0.72	0.71	0.08	3.07
PIN	RAN2804/511	t			0.86	1.08	1.26	0.46	0.87	0.59	0.21	3.37
<i>Edestus triserratus</i>												
GSM	31410	t		triser	1.84			0.92			0.54	5.90
TSNiGR	11/1865	t		minusc	1.35	1.40	1.04	0.59	1.23	0.48	0.17	
PIN	RAN2804/726	t		kolomn	3.45	3.80	1.10	2.16	2.66	0.81	1.14	
AMNH	485	w	l		3.04	3.36	1.11	2.05	2.72	0.75	0.64	11.86
n/a	Jillson [21]	w	u		3.71	3.19	0.86	1.84	2.56	0.72	0.63	14.58
CAS	n/a	w	u		2.93	3.27	1.12	1.95	2.47	0.79	0.21	14.98
FMNH	L309J865	t			2.73	2.64	0.97	1.64	2.48	0.66	0.16	9.07
FMNH	L309J872	t			1.56	2.22	1.42	1.16	2.03	0.57	0.19	7.59
FMNH	L310J870	t			1.86	1.97	1.06	1.10	1.80	0.61	0.17	
FMNH	L311J23	t			1.63	1.72	1.06	1.17	1.60	0.73	0.12	
FMNH	L312J852	t			1.67	2.16	1.29	1.13	2.03	0.56	0.13	8.78
FMNH	PF2317.1	w	l		2.72	2.40	0.88	1.60	1.97	0.81	0.43	9.50
FMNH	PF2317.2	w	l		2.47	2.40	0.97	1.40	1.89	0.74	0.51	9.80
FMNH	PF2317.3	w	l		2.69	2.51	0.93	1.68	1.98	0.85	0.53	
FMNH	PF2317.4	w	l		2.74	2.59	0.95	1.65	2.12	0.78	0.47	
FMNH	PF2317.5	w	l		2.60	2.49	0.96	1.60	2.15	0.74	0.34	
FMNH	PF2317.6	w	l		2.67	2.53	0.95	1.66	2.10	0.79	0.43	
FMNH	PF2317.7	w	l		2.48	2.47	1.00	1.68	2.10	0.80	0.37	
FMNH	PF2318	t			2.62	2.48	0.95	1.57	2.29	0.69	0.19	
FMNH	PF2319.1	t			3.07	3.12	1.02	1.71	2.63	0.65	0.49	11.48
FMNH	PF2319.2	t			3.99	3.29	0.82	2.04	2.78	0.73	0.51	11.01
FMNH	PF2319.3	t			3.32	3.43	1.03	2.16	2.87	0.75	0.56	9.49
FMNH	PF2326	t			2.39	2.45	1.03	1.53	2.31	0.66	0.14	
FMNH	PF2336	t			2.91	2.16	0.74	1.49	1.88	0.79	0.28	
FMNH	UC2092	t			2.98	2.80	0.94	1.46	2.28	0.64	0.52	11.47
FMNH	C67Dr15	t			2.37	2.20	0.93	1.31	1.79	0.73	0.41	
FMNH	HQ72	t			2.56	2.45	0.96	1.61	2.15	0.75	0.30	8.75

(Continued)

Table 3. (Continued)

Specimen		Elem	Posn	Type	Crown W	Crown H	Crown H:W	Crown uw	Crown uh	Crown uw:uh	Crown lh	Root L
USNM	14790	t			1.53	1.83	1.20	0.94	1.61	0.58	0.22	7.62

Teeth within a whorl are measured separately and their position in the whorl is annotated in the specimen identifier with a sequential decimal suffix (e.g., .1 is the anterior-most tooth, .2 is the adjacent tooth to the posterior, etc.). Type = Original species diagnoses: kolomn = *E. kolomnensis*; minor = *E. minor*; mirus = *E. mirus*; triser = *E. triserratus*; pring = *E. pringlei*; minusc = *E. minusculus*. Elem. = Element: t = tooth; w = whorl. Posn = Position: l = lower whorl; u = upper whorl. All tooth measurements presented in cm, and defined in Fig 1.

<https://doi.org/10.1371/journal.pone.0220958.t003>

corresponds to an anterior tilted apex, which distinguishes *E. protopirata* from other specimens. Crown width has a small positive correlation with PC1 ($r^2 = 0.25$, $t = 4.29$, p -value = 0.0001; excluding *E. giganteus* as an outlier) and crown width does not correlate with PC2 ($r^2 = 0.003$, $t = 0.386$, p -value = 0.69). Generally, with increased size, teeth are wider and shorter in shape. This observation is documented by consecutive crowns on a single whorl, as illustrated by five ANSP whorl specimens from a mine locality above the Herrin Coal (Fig 7B). Furthermore, crowns from these whorls span 0.5 units of the PC1 axis, and collectively span from -0.1 to +1.0, which includes all holotypes, but the outlier *E. giganteus*.

Analysis of the asymmetric specimens (Fig 8A and S2 Appendix) shows a reorientation of the PCs compared to analysis of all *Edestus* specimens (Fig 6). Positive PC1 (51% variance) corresponds to a stouter crown with an anterior tilt, and *E. kolomnensis* is the only holotype to have this aspect. There is no correspondence between size and PC1 ($r^2 = 0.019$, $t = 0.87$, p -value 0.38), and multiple crowns from a single whorl (e.g., FMNH PF 2319.1–3) show a broad range of nearly 0.2 along the PC1 axis. PC2, which accounts for 35% variance, distinguishes broad crowns in positive space versus crowns having a slender, bullet shaped outline in negative space. PC2 corresponds with size, and thus has potential to show an ontogenetic series. Plotting PC2 against crown width (Fig 8B) shows a weak positive correlation ($r^2 = 0.16$, $t = 2.80$, p -value = 0.0097), i.e., that as teeth grow wider at the base, the upper part of the crown also broadens. The positive correlation is stronger, however, if considering two distinct size-shape curves are represented in the graph, each resulting in adults with wider versus bullet-shaped crowns. Membership of upper and lower groupings are shown as convex hulls (Fig 8B). The upper grouping includes *E. mirus* and *E. minor* holotypes and *E. pringlei* at smaller size. The lower grouping includes *E. kolomnensis* in the large size, and *E. minusculus* at the smaller size, as well as crowns from the distinctive straight-whorled specimens of CAS and Jillson. Crowns from a single whorl, FMNH PF2317, appear intermediate between the main cluster of upper and lower groupings in Fig 8B, however they plot closer to lower grouping members in PC1-PC2 morphospace, thus our decision to include this specimen as part of the lower grouping.

The shape described by PC2 has a strong positive correlation ($r^2 = 0.84$, $t = 14.4$, p -value = 0.0001) with direct measures of the upper crown ratio (upper width by upper height) (Fig 8C). These direct measurements for the asymmetric specimens are plotted by crown width to reveal a similar pattern observed in the PCA: two ontogenetic series differing in the upper crown ratio by tooth width (Fig 8D). The holotype of *E. mirus* is significant in this sample because it illustrates overlapping upper ratios with variance of 0.1 and that lower crowns in this specimen are distinctly 0.5 cm narrower than upper crowns of the same individual. In nearly all specimens, using the crown upper ratio as a proxy for shape variance described by PC2 distinguishes membership of the upper versus lower groupings identified in Fig 8B. There is overlap in the upper ratio of three teeth between FMNH PF 2317 and the holotype of *E. mirus*, but this is small compared to the 0.2 upper ratio spread amongst all crowns of these two whorls.

The holotype of *E. triserratus* (GSM 31410) lacks the apex of the crown necessary for inclusion in the geometric analysis, however it does preserve the root and base of the crown up to the inflection points, allowing measurement of W, uw, and lh. Using the upper and lower groupings derived from the geometric analysis, we performed a discriminant analysis of linear measures to classify GSM 31410. The result classified GSM 31410 well within the lower grouping (Fig 8E), with an overall correct classification of 92.9%. Although this is not a statistical test, the close association of available measurements suggests the holotype of *E. triserratus* best fits among the lower grouping, which also corresponds to the original description of the species and inferred illustration by Newton ([23], Pl I.3) of a bullet-shaped asymmetric crown.

Summary of taxobases for *Edestus*. Results of geometric and traditional analyses identify crown shape as a primary taxobase, that when combined with root length and qualitative observations of whorl curvature distinguish four morphological concepts, redefined here to include *Edestus minor*, *E. triserratus*, *E. heinrichi*, and *E. vorax*. Classifying specimens within these new groups, we evaluated the original PCA for all specimens (Fig 6). Both PERMANOVA and ANOSIM suggest that each group is distinct, though we cannot resolve *E. vorax* ($n = 1$) with this approach (Table 4). *E. vorax* is distinct from *E. heinrichi* in terms of H:W and RootL:W (Fig 5 and Table 5).

Systematic Paleontology

Class Chondrichthyes Huxley, 1880 [24]

Subclass Euchondrocephali Lund and Grogan, 1997 [25]

Order Eugeneodontiformes Zangerl, 1981 [1]

Superfamily Edestoidea Hay, 1929 [26]

Family Edestidae Jaekel, 1899 [27]

Genus *Edestus* Leidy, 1856 [15]

Type species. *Edestus vorax* Leidy, 1856 [15]

Included species. *E. heinrichi*, *E. minor*, *E. triserratus*, *E. vorax*.

Diagnosis. Single symphyseal whorl in each upper and lower jaw, dimorphic, forming open spiral of up to 12 teeth, shed anteriorly; tooth crowns laterally compressed, triangular in shape with slightly concave edges bearing denticles; basal projection of crown directed posteriorly; elongate tooth roots stacked *en echelon* anteriorward along base of whorl opposite the crowns, whorl base has convex bulge.

Occurrence. Early to Middle Pennsylvanian (late Bashkirian to Moscovian). Britain, United States, Russia.

Remarks. The species *Lestrodus newtoni* Woodward, 1917 [28] (Obruchev, 1953 [11]) of the Namurian Millstone Grit Group (middle Morrowan age equivalent [12, 29]) is excluded from *Edestus*. The holotype of *L. newtoni*, GSM 28346, shows no evidence for a convex bulge opposite the tooth crowns on the whorl, a distinct feature common to all upper and lower whorls of *Edestus*. Furthermore, no clear evidence exists to demonstrate that *L. newtoni* had both upper and lower whorls. Three genera are formally synonymized under *Edestus*, following [7], including *Edestes* Miller, 1877 [30], *Edestodus* Obruchev, 1953 [11], and *Protospirata* Trautschold, 1888 [31].

Edestus minor Newberry in Newberry and Worthen, 1866 [32]

Fig 2C and 2F

Edestus minor Newberry in Newberry and Worthen, 1866 [32], pp. 84–85, pl. IV, Fig 24. Itano, 2014 [8], Figs 9 and 10.

Edestus mirus Hay, 1912 [5], p. 31–38, pl. 1–2.

Edestus pringlei Watson, 1930 [33], pp. 69–71, Fig 1A.

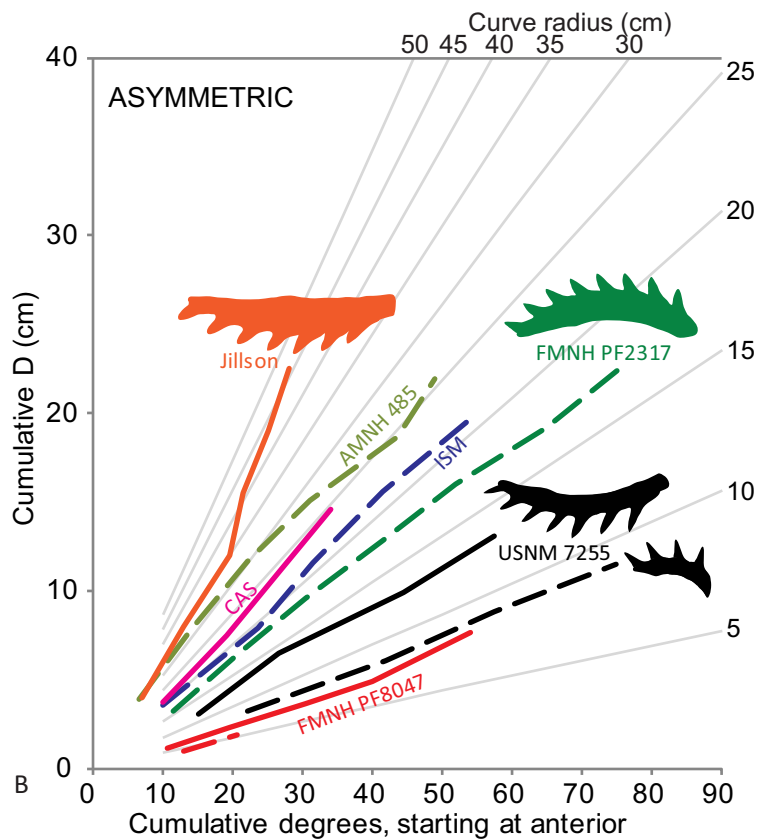
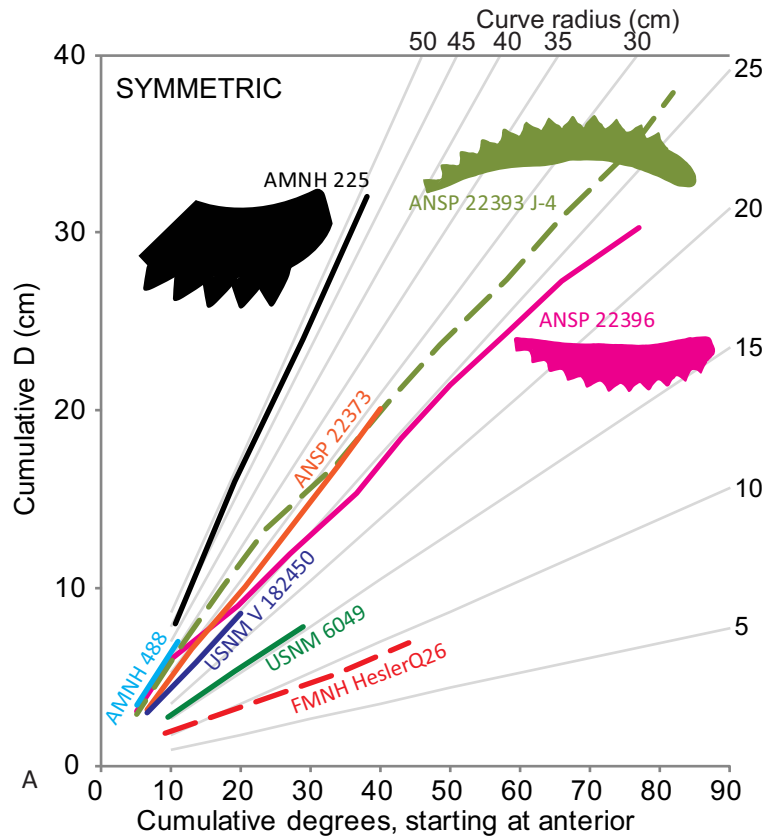


Fig 2. Four species of *Edestus*. (A) *E. heinrichi* crown, AMNH 466G. (B) X-ray of two small whorls of *E. heinrichi*, FMNH HQ 492 B-2. (C) *E. minor* crown, GSM 49368. (D) *E. triserratus* tooth, FMNH UC 2092. (E) *E. triserratus* tooth, GSM 31410. Scale bar same for A-E. (F) *E. minor* associated upper and lower whorls, USNM 7255; (G) X-ray of subadult *E. triserratus* associate upper and lower whorls with anterior jaws, FMNH PF 8047. Note two crowns lacking bases forming at posterior of upper whorl (arrow). (H) Adult *E. triserratus* upper whorl, CAS specimen, oriented with (I) similarly-sized lower whorl of *E. triserratus*, AMNH 485. (J) *E. heinrichi* whorl, AMNH 488 cast, plastotype. (K) *E. heinrichi* whorl, USNM V 182450. (L) *E. heinrichi* whorl, AMNH 6049. (M) X-ray of *E. heinrichi* whorl, FMNH HQ 26. (N) *E. heinrichi* tooth, FMNH HQ 1374 A3. (O) *E. vorax*, AMNH 225, note that all crown apices have been repaired. Scale bar same for G-O. Images C, E courtesy of British Geological Survey.

<https://doi.org/10.1371/journal.pone.0220958.g002>

Edestus minor Itano et al., 2012 [12], Fig 12.

Holotype. *E. minor*, AMNH FF477, Posey County, Indiana, age unknown.

Diagnosis. Obtuse triangular crown with gradual taper to apex, anteriorly; denticles fine; roots short in greatly curved lower whorl, moderate roots with slight curve in upper whorl.

Description. Crown height to width ratio near or above 1.0. Upper ratio ranges from 0.6 to 1.0 from juvenile ($W < 2\text{cm}$) to adult teeth ($W > 2\text{cm}$). The apical angle is approximately $30\text{--}35^\circ$. In adult crowns, fine denticles are $\sim 1\text{ mm}$ in width and may be subdivided by more than one cusp. USNM 7255 is the most complete example of the species, and demonstrates slight dignathism in size and shape of crowns of the upper and lower whorls. USNM 7255 (Figs 2F and 9) shows five lower crowns and a broken upper whorl with space for at least 6–8 crowns, and therefore may follow an 8:5 ratio for upper and lower whorl teeth. The convex bulge is conspicuous in the lower whorl of USNM 7255, and aligns with the junction of the symphysis of Meckelian cartilage preserved in the specimen. Crown morphology of the type AMNH FF477 most closely resembles an upper whorl tooth, but unfortunately the root is missing.

Other material examined. Six specimens including USNM 7255, GSM 49368, TMM 40234–8, and FMNH specimens HQ42, HQ435 B4, and HQ65.

Occurrence. Late Bashkirian to Moscovian. Westphalian B of Britain, Desmoinesian of U.S.A.

Remarks. The holotype specimen of *E. minor* (AMNH FF477, see [8], Figs 9 and 10) is a single crown and lacks most of the root. Newberry [32] described this holotype in the context of a separate 7-crown whorl (ACM 85 and its cast, AMNH 485, Fig 2I) first described by Hitchcock [34], noting that the latter was “similar, if not identical” to the holotype. Our geometric analysis demonstrates a fundamental shape difference between the two specimens despite their sizes being comparable. Instead, the holotype *E. minor* most closely resembles an upper whorl crown of USNM 7255, the holotype of *E. mirus*, which therefore becomes a junior synonym of *E. minor*.

Edestus triserratus Newton, 1904 [23] Fig 2D and 2E, Fig 2G–2I, Fig 3B, S1 Fig part *Edestus vorax* Newberry and Worthen, 1870 [13], pp. 353, pl. 1, Fig 2. Mistakenly identified.

Edestus triserratus Newton, 1904 [23], pp. 3–6, pl. I

Edestus minusculus Hay, 1909 [35], pp. 48–50, Fig 5. *E. cf. minor* Karpinsky, 1899 [3], p. 12–15, Figs 15–17, Pl. IV, Fig 12A–12C, 13.

Edestodus minusculus (Hay, 1909 [35]) Obruchev, 1953 [11] p. 52, Fig 24. 13 Lebedev, 2001 [14], pl. 44, Fig 4.

Edestodus kolomnensis (Lebedev, 2001 [14]), pl. 44, Fig 5.

Holotype. *E. triserratus*, GSM 31410, Westphalian B (upper Bashkirian), Staffordshire, England (Newton, 1904 [23]).

Diagnosis. Obtuse triangular crown narrowing to bullet-shaped apex, anteriorly; denticles fine; root proportionately longer than in *Edestus minor*; upper whorl with massive, straight base; lower whorl slender, more tightly curved.

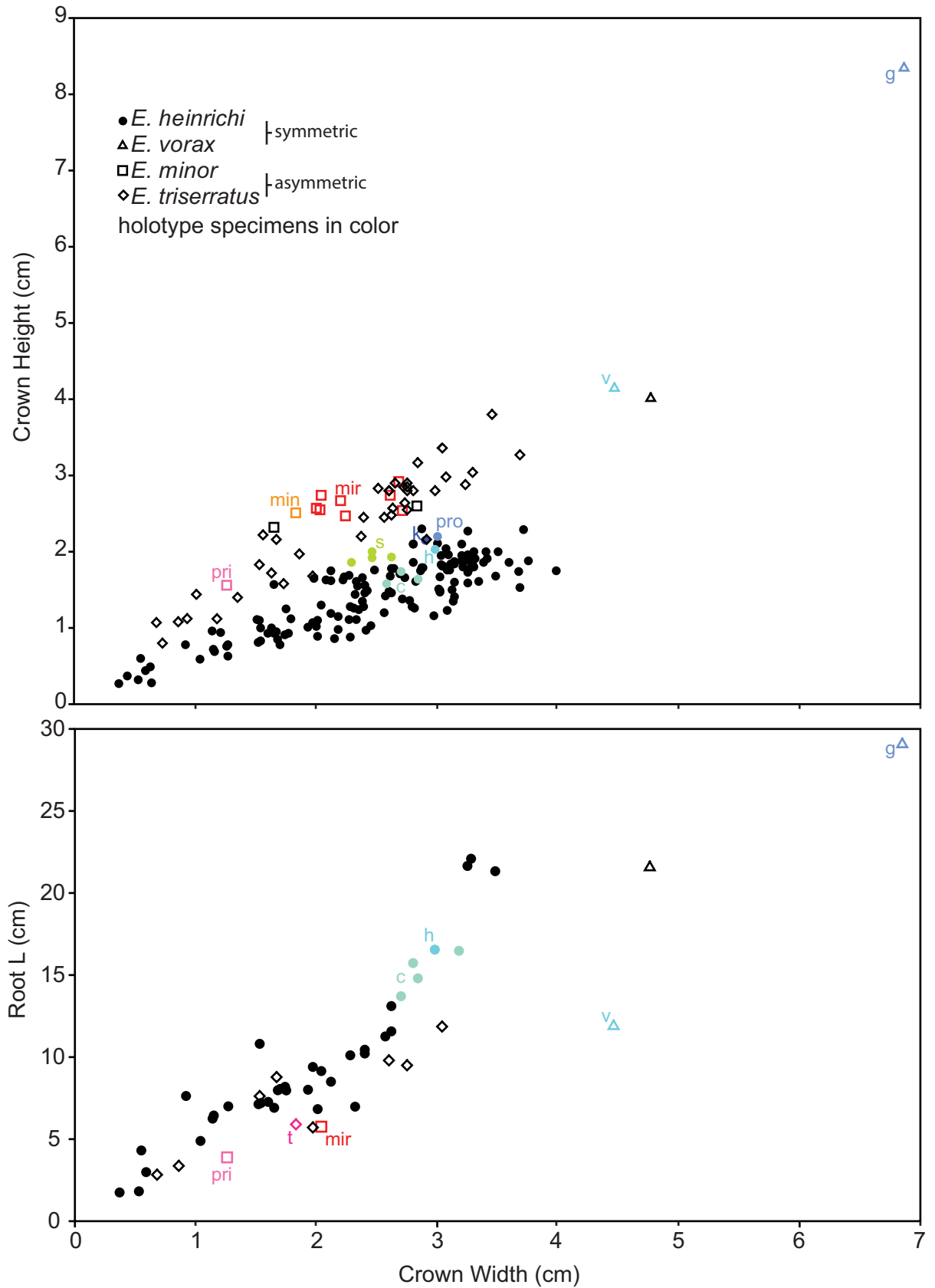


Fig 3. Upper and lower *Edestus* whorls. Renders from 3D laser scanned specimens. (A) *E. vorax* lower whorl, ANSP 9989, holotype. (B) *E. minor*, lower whorl, cast of FMNH PF 2317. (C) *E. heinrichi* upper whorl, ANSP 22391. (D) *E. heinrichi* upper whorl, ANSP 22392. (E) *E. heinrichi* upper whorl, ANSP 22396. (F) *E. heinrichi* lower whorl, ANSP 22373. (G) *E. heinrichi* lower whorl, ANSP 22393. Scale bar same for all.

<https://doi.org/10.1371/journal.pone.0220958.g003>

Occurrence. Late Bashkirian to Moscovian. Westphalian B of Britain; upper Atokan to Desmoinesian of United States (Colorado, Illinois, Indiana, Iowa, Kentucky, Oklahoma, Michigan, South Dakota, Texas); Myachkovian to ?early Krevyikian of Russia.

Description. Crown height to width ratio near or above 1.0. Upper ratio ranges from 0.5 to 0.8 from juvenile ($W < 2\text{cm}$) to adult teeth ($W > 2\text{cm}$). The apical angle is approximately 30–35°. In adult crowns, fine denticles are ~1 mm in width and may be subdivided by more than one cusp. Partially articulated cranial material with upper and lower whorls is known from FMNH PF 8047 (Figs 2G and 9). This specimen shows unrooted teeth at the posterior ends of the upper and lower whorls. The tooth count in this specimen shows 10 upper crowns and 6 lower crowns, but only 8 and 5, respectively, are rooted to the whorl. A lower adult whorl (ISM 497337, S1 Fig) similarly shows, at the posterior end of the whorl, a cluster of crowns most recently formed and have abbreviated roots. The upper whorl of the species, in adult form, is much less curved than its lower counterpart. The CAS specimen is a partly disaggregated whorl, when reconstructed shows very little curvature over the span of 8 crowns, and similarly, the whorl described and figured by Jillson [21] shows a nearly straight 7-crowned whorl of the species.

Other material examined. Includes 23 specimens, TSNiGR 11/1865, DMNH 61071, USNM14790, AMNH 485 (cast of ACM 85 Hitchcock), PIN RAN 2804/726, PIN RAN 2804/511, CAS specimen, Jillson specimen, ISM 497337, and FMNH specimens L309J865, L309J872, L310J870, L311J23, L312J852, PF2317, PF2318, PF2319, PF2326, PF2336, PF8047, UC2092, C67Dr15, and HQ72.

Remarks. Earlier diagnoses of *Edestus* species relied primarily on the number and division of denticles. For example, *E. triserratus* was designated for teeth with trifid denticles, whereas *E. pringlei* is bifid, and *E. minor* has both single and bifid denticles within the same whorl. There exists no accounting of variation within and across species concepts to validate denticle morphology as a discriminating variate. We therefore reject its use as a taxobase, in lieu of more readily quantified attributes presented in this study.

There is sufficient lower crown material of the holotype of *Edestus triserratus* to determine that the shape of the crown is pointing anteriorly and is approaching a bullet-shape. Discriminant analysis supports inclusion among this group of crown morphologies (Fig 8E).

Edestus triserratus differs from *E. minor* in crown proportions, most notably by being narrower and having subparallel anterior and posterior cutting edges toward the anterior-pointing apex. The posterior edge of the crown is longer and connects to the root at a shallower angle than in *Edestus minor*. This arrangement gives a wider space between individual teeth compared to *E. minor*. Whorls with *E. triserratus* crowns are either slightly curved or nearly straight. Although no articulated specimen of mature *E. triserratus* is yet known, it is reasonable that like other *Edestus* species, the straight whorl resides in the upper jaw and the lower whorl is slightly curved. Except for crown shape, the slightly curved lower whorl of *E. triserratus* and the slightly curved upper whorl of *E. minor* are not distinguishable. The crown arrangement of opposing whorls appear to mesh somewhat like gears near the middle part of the whorl (Fig 9). The degree of overlap (occlusion) is unknown in the species.

Edestus heinrichi Newberry and Worthen, 1870 [13]

Fig 2A and 2B, Fig 2J–2N, Fig 3C–3G

Edestus heinrichi Newberry and Worthen, 1870 [13], pp. 350–353, pl. 1, Fig 1A and 1B.

Edestus protopirata Trautschold, 1879 [15], p. 49–50, pl. 6, Fig 8. (Karpinsky, 1899) [3],

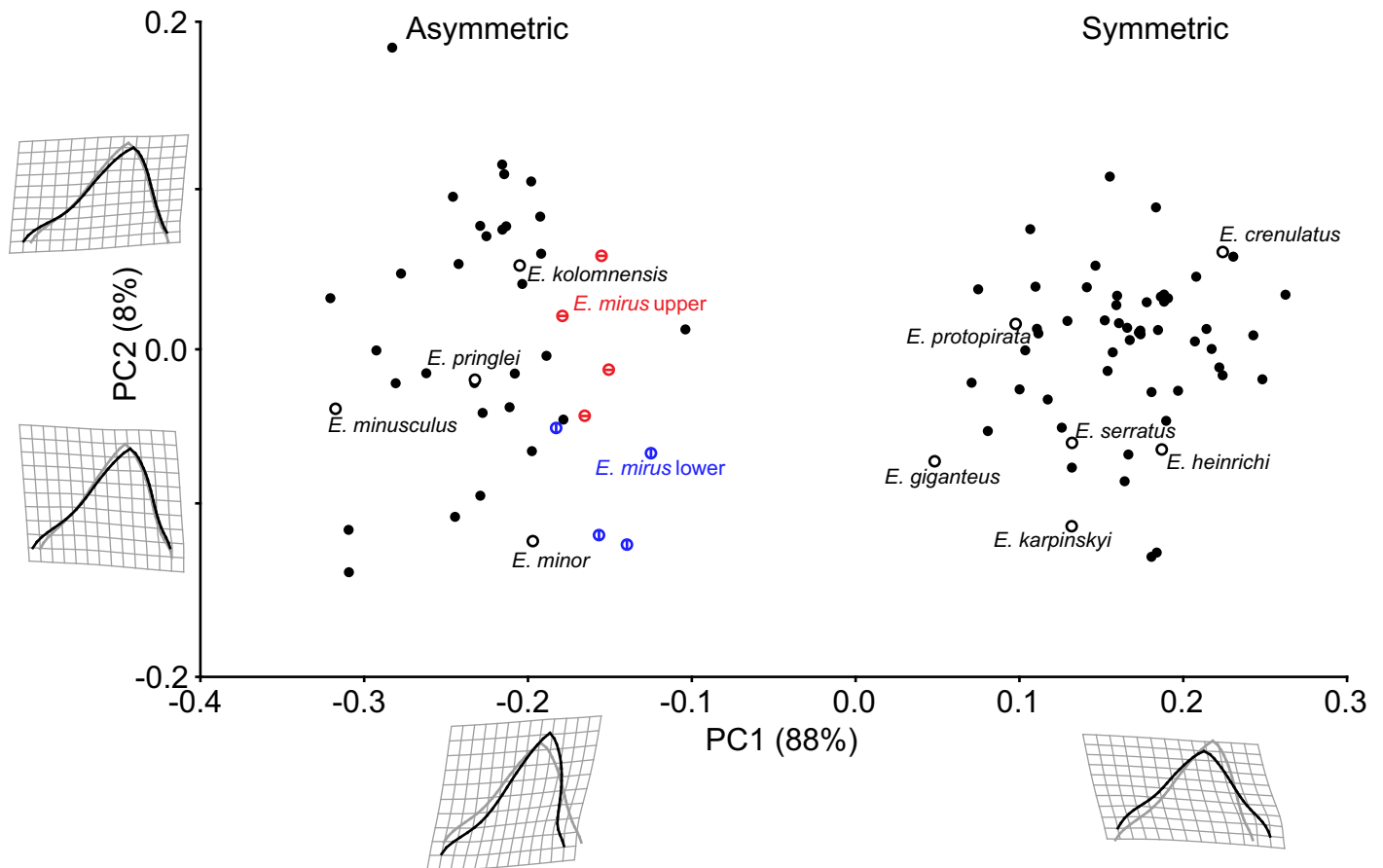


Fig 4. Occlusal curvature of *Edestus* tooth whorls. (A) Symmetric-crowned whorls. (B) Asymmetric-crowned whorls. Upper whorls have solid lines, lower whorls are dashed.

<https://doi.org/10.1371/journal.pone.0220958.g004>

Figs 6–7. *Protopirata centrodon* Trautschold, 1888 [31], p. 49. *Edestus karpinskyi* Missuna, 1908 [36], Figs 1–4. *Edestus crenulatus* Hay, 1909 [35], p.43–47, Figs 3 and 4, pl. 12, Figs 1–3. *Edestus serratus* Hay, 1909 [35], p. 47–48, Figs 3 and 4, pl. 12, Fig 4. *Protopirata protopirata* (Trautschold, 1879 [15]) Obruchev, 1953 [11], Pl.1, Fig 1, Pl. 2, Fig 1, Pl. 4, Fig 2. Lebedev, 2001 [14], pl. 44, Fig 8. *Protopirata karpinskyi* (Missuna, 1908 [36]) Obruchev, 1953 [11], Pl. 2, Fig 2, Pl 5, Fig 2. Lebedev, 2001 [14], pl. 44, Fig 7.

Holotype. *E. heinrichi*, whereabouts of original specimen unknown. In cases of a missing holotype specimen, the original illustration of the holotype (i.e., Newberry and Worthen, 1870 [13] pl. 1, Fig 1A and 1B) is designated as the name-bearing holotype (ICZN, 1999, Article 73.1.4)[20]. Casts of the holotype, such as AMNH FF 488, are considered plastotype material and do not constitute name-bearing type material (ICZN, 1999)[20].

Diagnosis. Crowns with acute triangular shape, with posterior edge slightly longer than anterior edge, large apical angle; denticles coarse; roots long and straight in upper whorl; slightly curved in lower whorl.

Occurrence. Moscovian. Carbondale Fm of United States (Desmoinesian); Mjachkovski horizon of Russia (Myachkovian to ?early Krevyaktion).

Description. Crown height to width ratio typically less than 1. Teeth from upper whorls have H:W above average (0.6–0.9) and lower whorl teeth are below average (0.4–0.6). The apical angle is roughly 80–85°. On 3 cm wide crowns, the coarse denticles measure roughly 2 mm

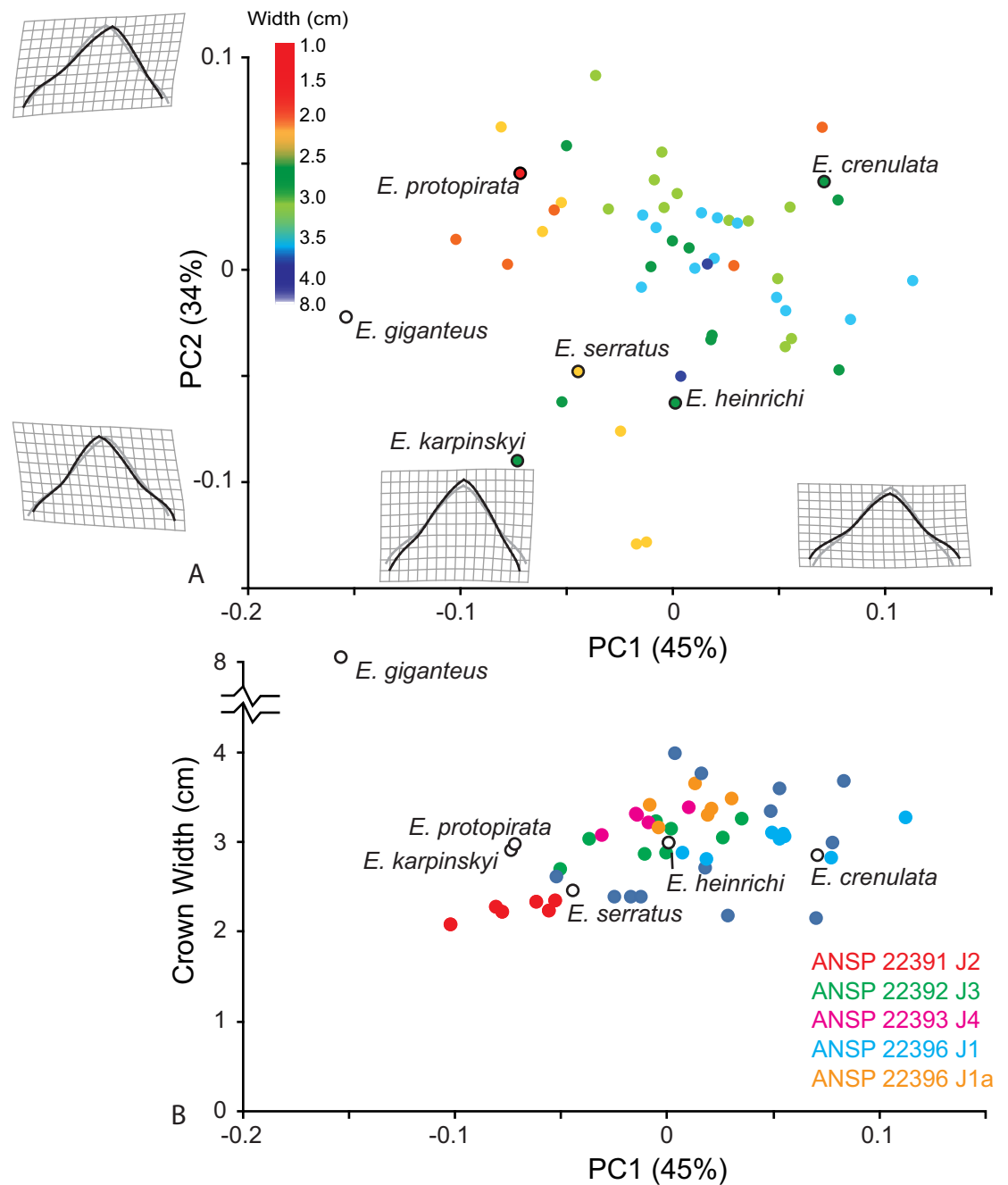


Fig 5. Crown dimensions for all studied *Edestus* specimens. Symbology corresponds to revised species designations. Holotype specimens of originally defined *Edestus* species have colored symbols; see Table 1 for specimen identification. Holotype abbreviations: c = *E. crenulatus*; g = *E. giganteus*; h = *E. heinrichi*; k = *E. karpinskyi*; min = *E. minor*; mir = *E. mirus*; pri = *E. pringlei*; s = *E. serratus*; t = *E. triserratus*; pro = *E. protopirata*; v = *E. vorax*.

<https://doi.org/10.1371/journal.pone.0220958.g005>

in width. Partly articulated cranial material from a juvenile, FMNH PF 2204, shows upper and lower whorls in context ([6], Fig 1; [2]), with at least 8 upper crowns and 5 lower crowns per whorl. Juvenile tooth roots are longer in the upper whorl and form a more massive whorl in comparison to the slender lower whorl. In larger specimens from the Jeremiah collection, the

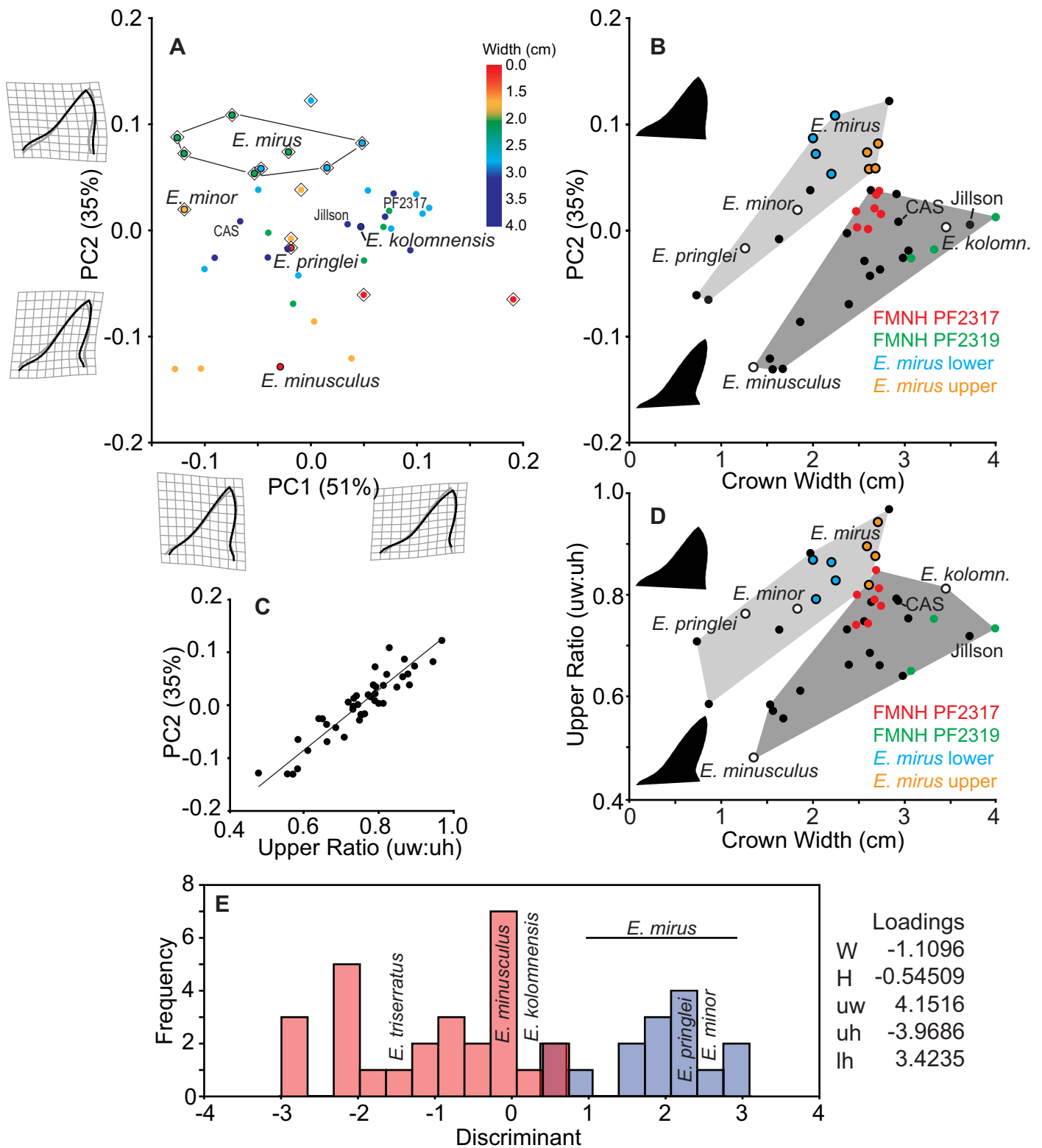


Fig 6. Geometric morphometrics of all *Edestus* specimens. Type specimens are outlined with black circles. Holotype *E. mirus* crowns from upper and lower whorls shown in red and blue circles, respectively.

<https://doi.org/10.1371/journal.pone.0220958.g006>

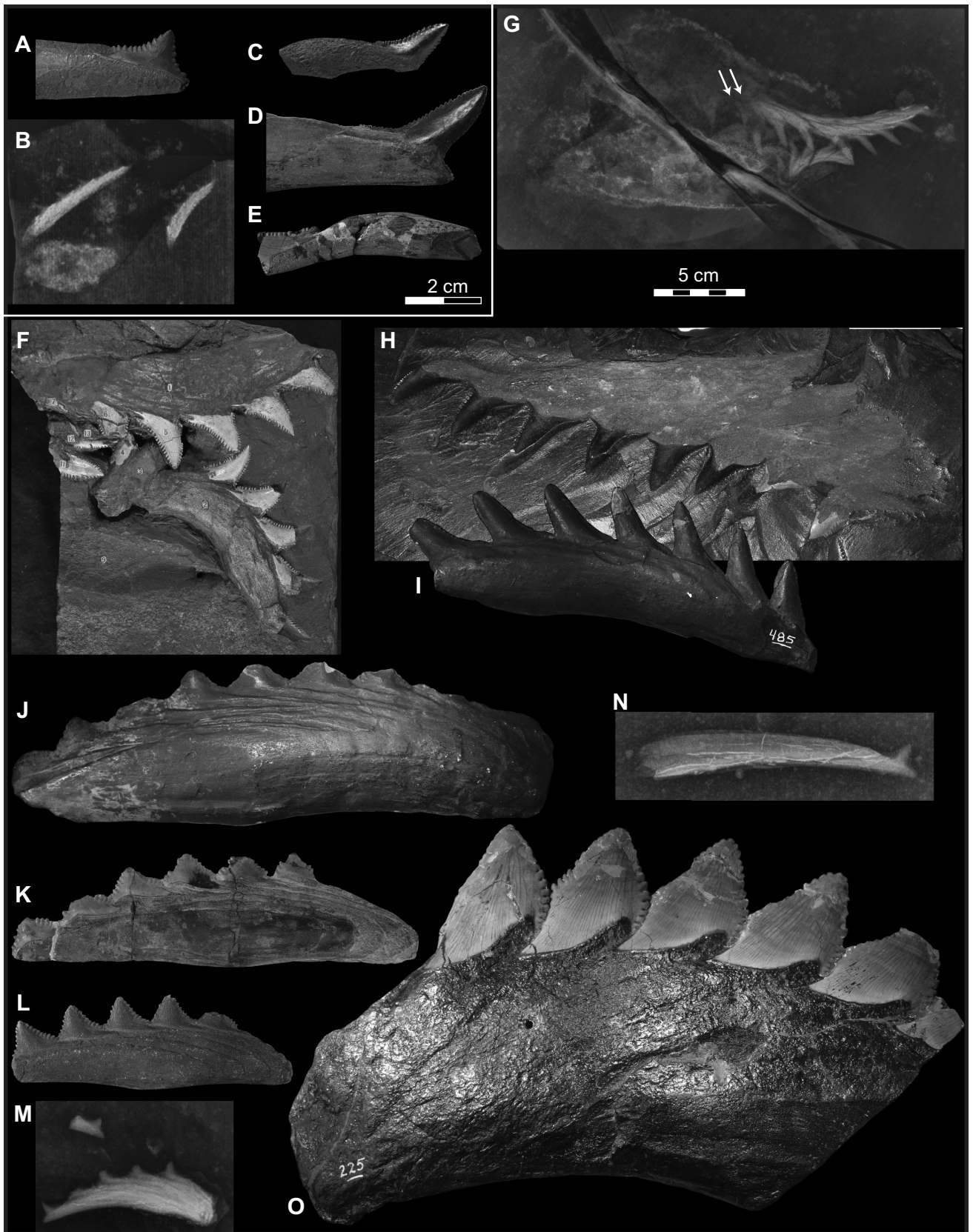


Fig 7. Geometric morphometrics of *Edestus* with symmetric-crowned teeth. (A) PCA of all crowns color-coded by crown width size to show ontogenetic variation. Holotypes have outlined circle symbol. (B) Five whorls from ANSP provide PC1 shape of consecutive crowns plotted by crown width. Holotypes have outlined circles filled white. Note significant outlier *E. giganteus* holotype above the y-axis excursion.

<https://doi.org/10.1371/journal.pone.0220958.g007>

more massive base of the upper whorl contrasts the slender profile of the lower whorl. Both whorls have strongly curved occlusal surfaces (Fig 9). The opposite surface, formed by the overlapping of V-shaped roots, is nearly straight in the upper whorl, whereas in the lower whorl, it forms a concave curve nearly parallel to the occlusal curve. Refer to [2] for description of a juvenile skull of this species.

Other material examined. Includes 106 specimens, USNM V 182450 (6050), USNM 6049, PIN RAN 1988 /2, Trautschold, 1879 specimen, PIN RAN 1988/1; specimens from ANSP include 22376, 22378, 22379, 22380, 22381, 22382, 22383, 22384, 22387, 22390, 22398, 22399, 22400, 22401, 22402, 22403, 22404, 22405, 22406, 22412, 22413, 22414, 22415, 22416, 22417, 22418, 22419, 22420, 22423, 22424, 22425, 22426, 22428, 22430, 22431, 22433, 22435, 22436, 22377, 22411, 22391, 22392 J-3, 22396 J-1, 22373 J-5, 22393 J-4; specimens from FMNH include Barret #6, C67 Dr 15–4, CompPenn#17, HQ26, HQ114, HQ1329 B-1, HQ1344-B-2, HQ46, HQ554 A-2, HQ555 B-1, HQ610 A-3, HQ66, HQ69,70(B), HQ799 B-1, HQ983 A-2, Jelliff#2, L238, L250, L309 (J864), L310 (J629), L310 (J859), L311 (J1068), L311 (J288), L311 (J938), L312(J61), L314, 315A(PF2320), L316, L317(2314), Logan 115 (J657), MontgomeryCk dr5, MQ236 (PF2852), PF2320, PF-2323, PF-2330, PF2331 J-122, PF2335 J288, PF-2339, PF-2341, PF-8049, PF-8404, Pit 14(17&18), Pit 14(Peabody Coal), Q208, UC3316, C67 Dr 15–1, C67 Dr 15–3, CompPenn#19, Fish pit 12, HQ1374 A-3, PF-1024, X-Ray #10, PF-2845, PF-8735, UF30, HeslerQ 26.

Remarks. Teeth in an anterior position on the whorl have longer roots than those at the posterior end, e.g., USNM 6049, ANSP 22392 J3 (Fig 3D), and FMNH PF 8735. This pattern demonstrates that the posterior root of a tooth continues to grow and results in the anterior advancement of teeth in the whorl. In the course of its travel to an anterior position, but prior to being ejected, the root stops elongating. The whorl, ANSP 22396 J1 (Fig 3E), shows this with equivalent lengths of the four anterior teeth. Once fully formed, ejected teeth and anterior teeth of whorls share similar root length proportions. By contrast teeth in posterior positions of the whorl have stunted root proportions and crown dimensions tend to plot higher than average (Fig 5).

Edestus vorax Leidy, 1856 [16]

Figs 2O and 3A.

Edestus vorax Leidy, 1856 [16], pp. 159–160, pl. 15, Figs 1–4.

Edestus giganteus Newberry, 1889 [37], pp. 225–226, pl. XL.

Holotype. *E. vorax*, ANSP 9899 (Leidy, 1856) [16], Muskogee Co., Oklahoma [10], Desmoinesian.

Diagnosis. Crowns with acute triangular shape, with slightly longer posterior edge, intermediate apical angle; denticles very coarse; roots stout and extend deep below crown.

Occurrence. Moscovian. Desmoinesian of United States.

Other material examined. Includes four specimens, AMNH 225, KGS specimen, FMNH UC 14346, and USNM 330005.

Description. Dimensions are presented in Table 2. Crown height to width ratio greater than 0.9. Denticles wider than 2 mm. Apical angle of roughly 65°.

Remarks. The similarity of *E. vorax* and *E. giganteus* was recognized by Branson [10], though subsequent authors have not followed his recommendation for synonymy. Little is known about *E. vorax* due to its sparse fossil record (n = 5), and therefore variation within the

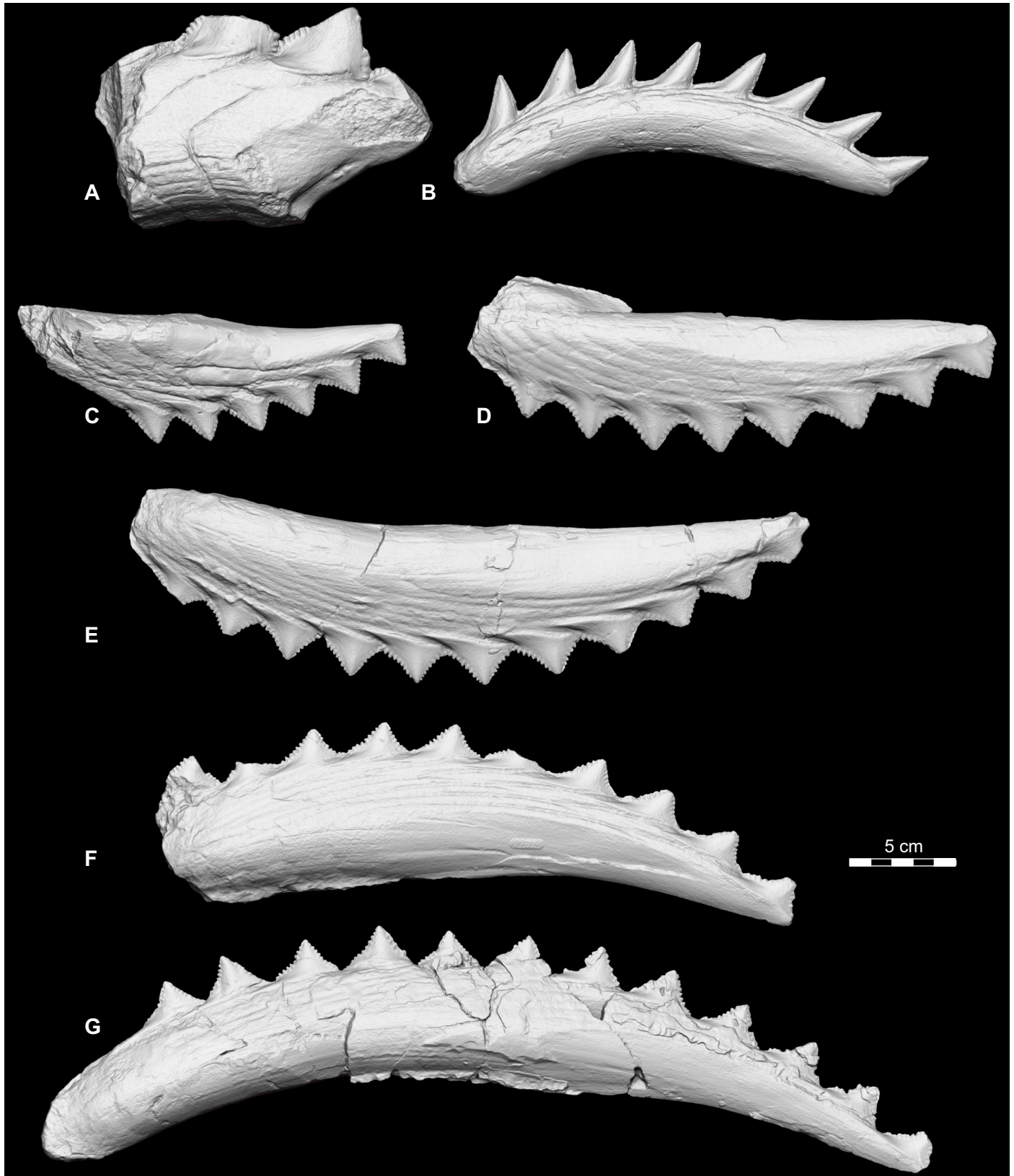


Fig 8. Geometric morphometrics of *Edestus* with asymmetric-crowned teeth. (A) PCA of all crowns color-coded by crown width size to show ontogenetic variation. Multiple crowns from holotype *E. mirus* from both upper and lower whorls outlined. All holotypes have black outlined circle symbol. Diamond symbol denotes specimens plotted in the upper grouping of B. (B) PC2 plotted by crown width. Light and dark grey convex hulls demark morphospace of two groups of crowns. (C) PC2 of all asymmetric crowns correlates strongly with the upper ratio metric. (D) Ratio of linear measures distinguishing two asymmetric crown types for *Edestus*, based on geometric ordination and groupings in B. (E) Discriminant analysis of asymmetric crown using linear measurements classified by groupings shown in B and D. Holotype specimens of *E. triserratus*, *E. minusculus*, and *E. kolomnensis* form the upper group (pink); Holotypes of *E. mirus* (multiple crowns), *E. pringlei*, and *E. minor* form lower group (blue). Loadings for linear measurements (see Fig 1) on the discriminant axis.

<https://doi.org/10.1371/journal.pone.0220958.g008>

species and its ontogeny remains under-sampled. The convex bulge is conspicuous on the KGS and AMNH 225 whorls, hence its inclusion in the genus. Dimorphism in upper and lower whorls is expected, but currently unknown (Fig 9). Itano et al. [12] have suggested that *E. vorax* is a large individual equivalent to *E. heinrichi*. The measurements in this study unequivocally reject this hypothesis. Ontogenetic series of *E. heinrichi* crown height, for example, follows a trajectory (Fig 5), that steepens at roughly 2.3 cm, far short of *E. vorax* crowns known to be beyond 8 cm tall. One could still argue that juvenile *E. vorax* with smaller crowns must exist, yet the *E. heinrichi* population studied here cannot account for short, greatly thickened root structures found in all *E. vorax*. As *E. heinrichi* whorls get larger during ontogeny, their roots consistently elongate posteriorly relative to their crowns with no evidence for a shift toward shortening and thickening with increased crown size. Growth trends documented here strongly support *E. vorax* as a separate species.

Discussion

The largest dataset yet compiled of *Edestus* teeth provides a quantitative foundation for defining species concepts that incorporate ontogeny and disparities associated with upper and lower dentitions. As found with the edestoid, *Helicoprion* [9], we find species diversity to be substantially decreased when morphometric methods are applied to larger datasets. The four distinct morphological species defined here provide new constraints on the morphology, size, and geographic history of *Edestus* when placed in context of the recently described cranium and jaw of a juvenile *Edestus heinrichi*, FMNH PF 2204 [2].

Table 4. Nonparametric tests for new groupings of *Edestus* specimens from principle components analysis. Results of PERMANOVA ($F = 174.9$, $p = 0.0001$) and ANOSIM ($R = 0.93$, $p = 0.0001$).

PERMANOVA			
p-values	<i>E. triserratus</i>	<i>E. heinrichi</i>	<i>E. vorax</i> ($n = 1$)
<i>E. minor</i> ($n = 11$)	0.0006*	0.0006*	0.5154
<i>E. triserratus</i> ($n = 31$)		0.0006*	0.2004
<i>E. heinrichi</i> ($n = 55$)			0.1068
F-values			
<i>E. minor</i>	11.9	169.1	8.433
<i>E. triserratus</i>		459.9	10.88
<i>E. heinrichi</i>			4.824
ANOSIM			
p-values			
<i>E. minor</i>	0.0015*	0.0003*	—
<i>E. triserratus</i>		0.0003*	—
R-values			
<i>E. minor</i>	0.3323	0.9996	—
<i>E. triserratus</i>		0.9999	—

*p-values significant, suggesting *Edestus* groupings occupy different morphospaces.

<https://doi.org/10.1371/journal.pone.0220958.t004>

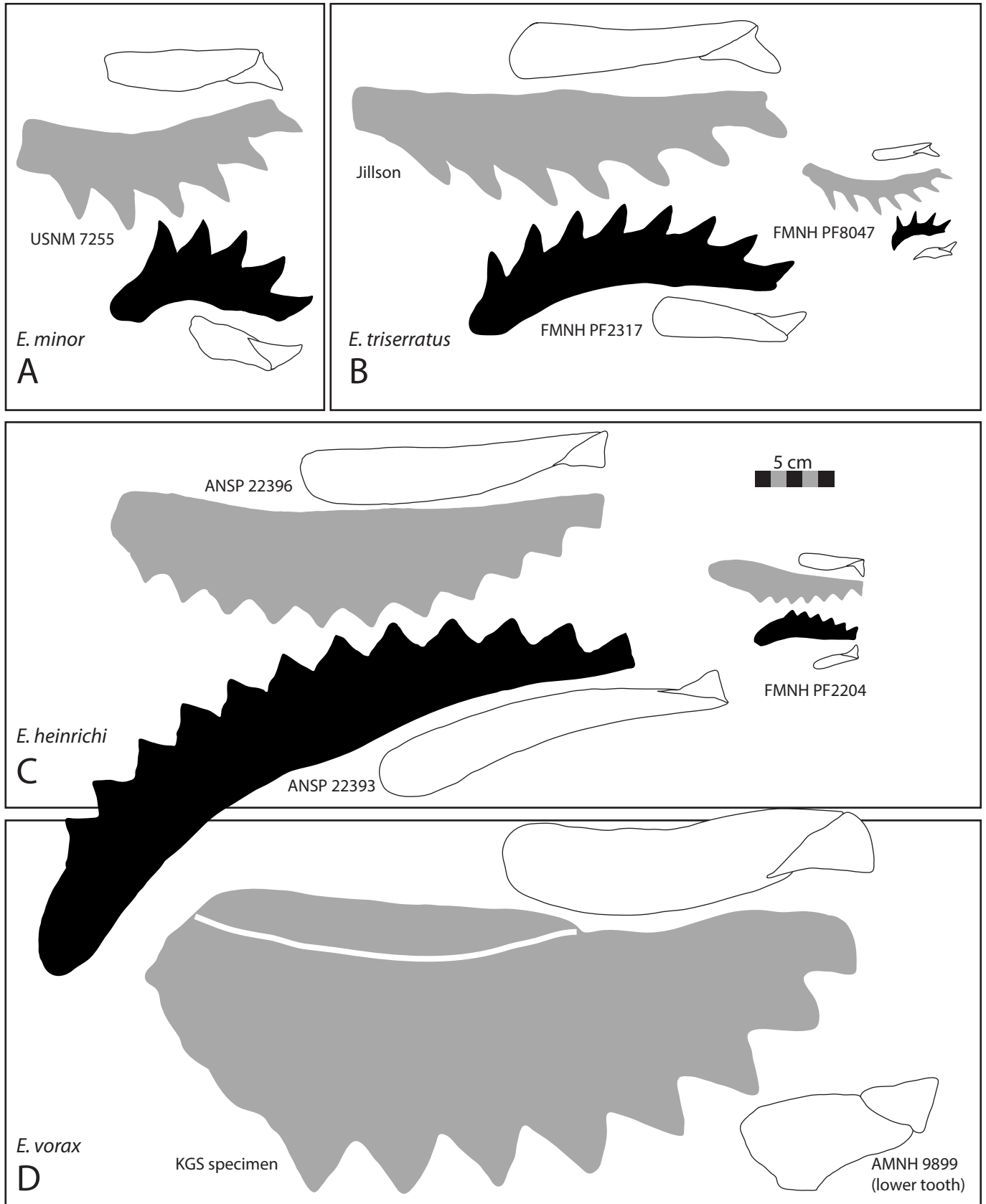


Fig 9. Illustration of revised *Edestus* species whorls and teeth. (A) *Edestus minor* represented by associated upper and lower whorl. (B) *Edestus triserratus* adult represented by two separate specimens of compatible size, and subadult represented by associated upper and lower whorls. (C) *Edestus heinrichi* adult form represented by two separate specimens of compatible size, and subadult represented by associated upper and lower whorls. (D) *Edestus vorax* adult upper whorl and lower tooth of separate individual. Scale bar for all specimens.

<https://doi.org/10.1371/journal.pone.0220958.g009>

Analysis of *E. heinrichi* (FMNH PF 2204) demonstrated that the opposing tooth whorls functioned as grasping and slicing tools. As the lower jaw closes toward the fixed upper whorl, it moves anterodorsally, causing teeth to slice for up to three tooth-lengths through the prey item. As the mouth re-opens, jaw depressors pull the lower jaw posteroventrally, providing a second slicing motion of teeth through the prey. Upper and lower teeth do not shear past one another in a “true” scissor-like motion, but rather stop short and remain parallel during the bite sequence. Given the similar shape of the whorls through ontogeny, it is parsimonious to expect similar jaw mechanics in the adult *E. heinrichi*.

Furthermore, extrapolating the anatomy and joints of the *E. heinrichi* jaw to the other three species is regarded here as reasonable, with some consideration. The asymmetric species *E. triserratus* and *E. minor* have whorls that exhibit a greater degree of curvature, leading Itano [8, 38, 39, 40] to imagine the whorls to curl outside the mouth for a vertical slashing motion. The evidence used for this hypothesis include several specimens of *Edestus* teeth showing wear patterns that are predominantly transverse to the crown (i.e., parallel to the base) [38, 39, 40]. This wear pattern is entirely consistent with the anatomy and functional reconstruction of FMNH PF 2204 [2], showing that *Edestus* whorls were positioned in opposition inside the mouth, and that the biting motion involved anterior-posterior slicing with the lower whorl. Furthermore, transverse wear patterns are found on both asymmetric and symmetric species, implying that slicing is the common mechanism for biting in all *Edestus*.

Using the jaw of *E. heinrichi* as a conservative model, whorls of the asymmetric species, when scaled for size, fit easily within the supporting palatine and Meckel’s cartilages. We might anticipate a shortening of the lower jaw in *E. minor* to take advantage of the greater occlusal curvature to generate more slicing action, as found in the short jaw of *Helicoprion* [41]. *Edestus vorax* has a substantially more robust tooth whorl and would necessitate an equally robust jaw structure to accommodate its greater size. Beyond variations in proportions, we regard the jaw morphology observed in *E. heinrichi* (FMNH PF 2204) as conservative within the genus, pending new discoveries of *Edestus* cranial material.

FMNH PF 2204 also provides some rough estimation for maximum body size in *E. heinrichi*. The upper and lower whorls of FMNH PF 2204 measure 10.4 cm and 8 cm, respectively, and are contained within a cranium roughly 25 cm in length. The largest individual *E. heinrichi* whorls include an upper whorl measuring 32 cm (ANSP 22396, Fig 3E) and a lower whorl measuring 43 cm (ANSP 22393, Fig 3G). Assuming isometric growth, which is a conservative underestimation given the positive allometry found in *Helicoprion* [9], the cranium of *Edestus heinrichi* attained minimum lengths of 77 to 134 cm for these two specimens, respectively. Using a conservative 5:1 body to head length ratio allows a minimum rough estimate of *E. heinrichi* body length of 6.7 m (Fig 10).

The consolidation of species provides some insight on the timing and geographic expansion of *Edestus*. The history of the group is recorded in paleoequatorial to tropical latitudes (Fig 11). Transgressive marine shale deposits overlying coal swamps are the most frequent depositional setting for *Edestus*, with relatively few reported from basinal marine limestones. *Lestrodus newtoni*, whose root and crown morphology bears closest resemblance to *Edestus*, precedes it in Britain during the Namurian regional stage (middle Bashkirian, early Pennsylvanian). The first *Edestus* species have asymmetric crowns and include both *E. minor* and *E. triserratus* in the Westphalian B (latest Bashkirian) coastal marine deposits of England. By Moscovian time,

Table 5. Crown height to width ratio for new *Edestus* groupings. Results of ordinary least squares regression of log-transformed values.

H : W	<i>E. minor</i>	<i>E. triserratus</i>	<i>E. heinrichi</i>	<i>E. vorax</i>
N	12	40	149	3
Min	0.92	0.74	0.39	0.85
Max	1.41	1.57	1.09	1.22
Mean	1.19	1.06	0.60	1.00
Stand. dev	0.16	0.16	0.12	0.20
Median	1.23	1.05	0.59	0.93
logH : logW OLS				
Slope a	1.195	1.1303	0.9518	
Intercept b	-0.1468	-0.0646	0.2349	
R ²	0.6484	0.9044	0.8147	
t	4.2947	18.964	25.421	
p-value	0.0024	0.0001	0.0001	

<https://doi.org/10.1371/journal.pone.0220958.t005>

uplift associated with the Variscan orogeny shifts much of Britain's depositional environments to alluvial facies [42], and no further *Edestus* fossils are found in the region. Elsewhere, *Edestus* diversified and expanded their range to include the Russian Platform and central United States

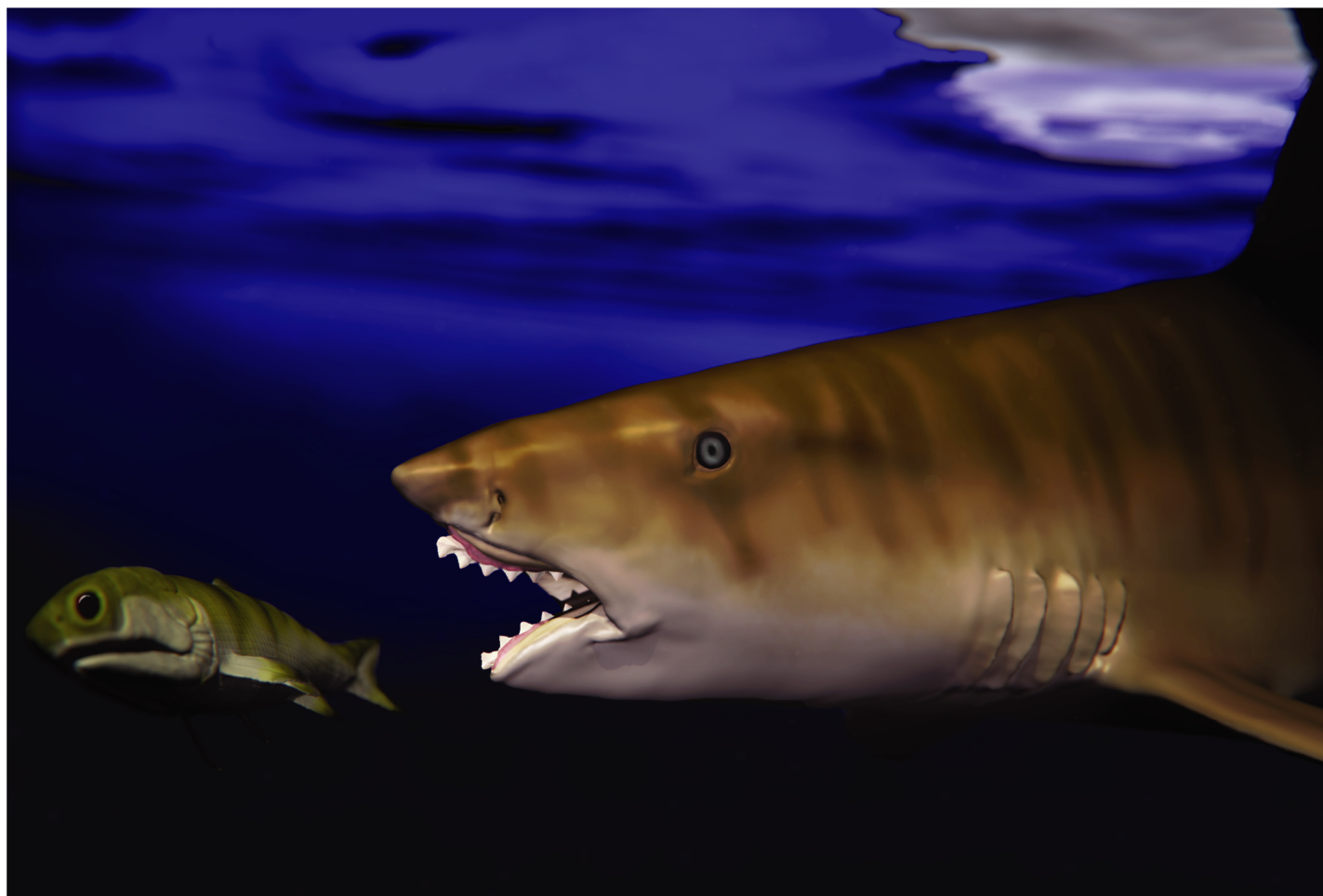


Fig 10. *Edestus heinrichi* preying on a palaeoniscoid fish. 3D illustration by Jesse Pruitt and Evelyn Vollmer, Idaho Virtualization Lab.

<https://doi.org/10.1371/journal.pone.0220958.g010>

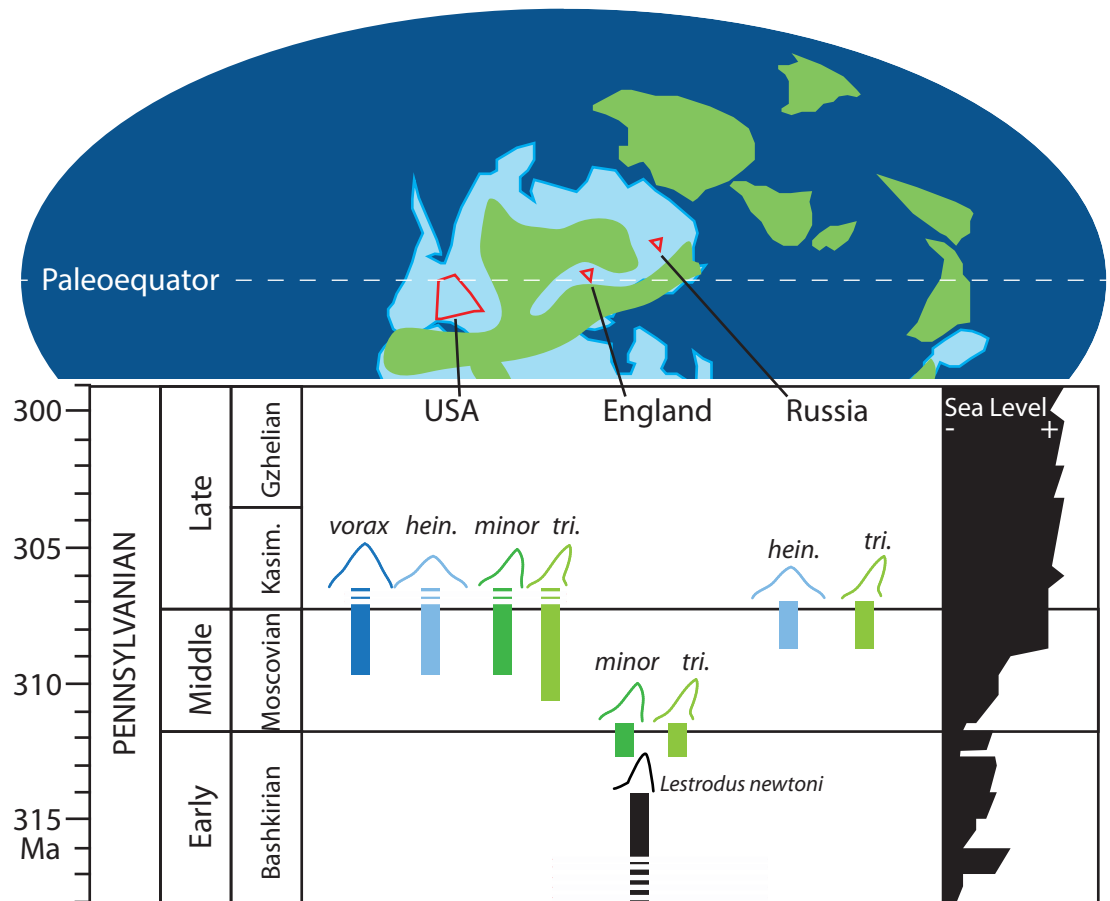


Fig 11. *Lestrodus* and *Edestus* in space and time. Paleogeographic map for the Middle Pennsylvanian modified from [43] and sea level curve modified from [44]. Uncertainty in species range shown with dashed boxes. Abbreviations: Kasim. = Kasimovian; vorax = *Edestus vorax*; hein. = *Edestus heinrichi*; minor = *Edestus minor*; tri. = *Edestus triserratus*.

<https://doi.org/10.1371/journal.pone.0220958.g011>

coincident with the global Moscovian transgression. *Edestus heinrichi* and *E. triserratus*, as revised here, are found in deposits of regional Myachkovian age, whereas all four *Edestus* species are found in Atokan to Desmoinesian marginal marine deposits in the US. No *Edestus* are reported after the Desmoinesian, suggesting that their stratigraphic range is from late Bashkirian to Moscovian, approximately 313 to 307 Ma.

Supporting information

S1 Appendix. Spreadsheet for principle components analysis for symmetric crowns depicted in Fig 7A.
(XLSX)

S2 Appendix. Spreadsheet for principle components analysis for asymmetric crowns depicted in Fig 8A.
(XLSX)

S1 Fig. Line drawings of *Edestus triserratus* whorls. (A) ISM 497337, lower whorl. (B) Jillson specimen, upper whorl.
(EPS)

Acknowledgments

We are grateful for the enthusiasm shared by R. Troll for these fossils and for introducing us to Zangerl's collection and correspondence. ISU undergraduate, N. Corder, helped measure tooth x-rays from the FMNH collections. We thank our museum colleagues for providing access, images, and loans for this project: A. Gishlick (AMNH), W. Simpson (FMNH), D. Bohaska (NMNH), P. Shepherd (British Geological Survey), T. Daeschler (ANSP), O. Lebedev (PIN), D. Roberts, C. Widga and D. Roberts (CAS), and K. Wellspring (ACM). We appreciate thorough reviews by C. Underwood, J. Kriwet, and an anonymous reviewer, whose critiques helped sharpen our arguments.

Author Contributions

Conceptualization: Leif Tapanila, Jesse Pruitt.

Data curation: Leif Tapanila.

Formal analysis: Leif Tapanila.

Investigation: Leif Tapanila.

Methodology: Leif Tapanila, Jesse Pruitt.

Project administration: Leif Tapanila.

Resources: Leif Tapanila.

Software: Jesse Pruitt.

Supervision: Leif Tapanila.

Validation: Leif Tapanila.

Visualization: Leif Tapanila, Jesse Pruitt.

Writing – original draft: Leif Tapanila.

Writing – review & editing: Leif Tapanila.

References

1. Zangerl R. Chondrichthyes I. Paleozoic Elasmobranchii. Handbook of Paleichthyology, 1981; 3A, Gustav Fischer, New York, 113 p.
2. Tapanila L, Pruitt J, Wilga CD, Pradel A. Saws, scissors and sharks: Late Paleozoic experimentation with symphyseal dentition. *Anat Rec*, 2018; <https://doi.org/10.1002/ar.24046> PMID: 30536888
3. Karpinsky AP. Über die Reste von Edestiden und die neue Gattung *Helicoprion*. *Verh Russisch-Kaiserlichen Mineralogischen Gesellschaft*, 1899; 36:361–475.
4. Tapanila L, Pruitt J, Pradel A, Wilga CD, Ramsay JB, Schlader R, et al. Jaws for a spiral-tooth whorl: CT images reveal novel adaptation and phylogeny in fossil *Helicoprion*. *Biol Letters*, 2013; 9:20130057.
5. Hay OP. On an important specimen of *Edestus*; with description of a new species, *Edestus mirus*. *Proc US Nat Mus*. 1912; 42:31–38.
6. Zangerl R, Jeremiah C. Notes on the tooth "saw blades" of *Edestus*, a late Paleozoic chondrichthyan. *Mosasaur*, 2004; 7:9–18.
7. Ginter M, Hampe O, Duffin C J. Chondrichthyes. Paleozoic Elasmobranchii: Teeth. Handbook of Paleichthyology, 2010; v. 3D: Munich, Verlag Dr. Friedrich Pfeil, 168 p.
8. Itano WM. *Edestus*, the strangest shark? First report from New Mexico, North American paleobiogeography, and a new hypothesis on its method of predation. *Mountain Geologist*, 2014; 5:201–221.
9. Tapanila L, Pruitt J. Unraveling species concepts for the *Helicoprion* tooth whorl. *J Paleontol*, 2013; 87:965–983.
10. Branson CC. Type species of *Edestus* Leidy. *Oklahoma Geology Notes*, 1963; 23: 275–280.

11. Obruchev DV. Edestid studies and the works by A. P. Karpinsky. Trudy Paleontologicheskogo Instituta Akademii Nauk SSSR, 1953; 45:1–85.
12. Itano WM, Houck KJ, Lockley MG. Systematics and occurrences of *Edestus* (Chondrichthyes) worldwide and new occurrences from Colorado and Texas. Hist Biol. 2012; 24: 397–410.
13. Newberry JS, Worthen AH. Descriptions of vertebrates. Geol Surv Illinois, 1870; 4:343–374.
14. Lebedev OA. Chapter 14. Pozvonochnye, in Makhlina MK, Alekseev AS, Goreva AS, Gorjunova RV, Isakova TN, Kosovaya OL, et al. eds., Srednij karbon Moskovskoy sineklizy (yuzhnaya chast') Tom 2. Nauchnyi Mir, Moscow, 2001; 196–201.
15. Trautschold H. Die Kalkbrüche von Mjatschkowa. Eine Monographie des oberen Bergkalks. Nouveaux Mémoires de la Société Impériale des Naturalistes de Moscou, 1879; 14:1–82.
16. Leidy J. Descriptions of some remains of fishes from the Carboniferous and Devonian formations of the United States. J Acad Nat Sci Philadel. 1856; 3:159–165.
17. Zangerl R, Richardson ES. The paleoecological history of two Pennsylvanian black shales. Fieldiana Geol Memoir, 1963; 4:1–352.
18. Koenig JW. Midcontinent Pennsylvanian Edestidae. Report of Investigations—Missouri Geol Surv Water Resources, 1965; 33:1–25.
19. Richards BC. Current status of the international Carboniferous time scale. New Mexico Mus Nat Hist Sci Bull. 2013; 60:348–353.
20. ICZN. International Code of Zoological Nomenclature. 1999; Fourth edition. London, U.K. [available online at <http://www.iczn.org/iczn/index.jsp>]. International Trust for Zoological Nomenclature.
21. Jillson WR. *Edestus minor*: an extinct shark from the Allegheny Series of western Kentucky. 1949; Roberts Printing Co., Frankfort, KY, 16 p.
22. Greb S, Weisenfluh J, Etensohn F, Ciampaglio C. *Edestus giganteus* shark fossils from the Carboniferous Formation (Middle Pennsylvanian, Desmoinesian), western Kentucky, Illinois Basin. Abstract for the 2011 annual meeting of the Kentucky Academy of Science, 2011; Murray State University, Murray (KY).
23. Newton ET. On the occurrence of *Edestus* in the Coal-Measures of Britain. Q J Geol Soc London, 1904; 60:1–9.
24. Huxley TH. On the application of the laws of evolution to the arrangement of the Vertebrata and more particularly the Mammalia. Proc Zool Soc London. 1880; p. 649–662.
25. Lund R, Grogan ED. Relationships of the Chimaeriformes and the basal radiation of the Chondrichthyes. Rev Fish Biol Fisher. 1997; 7:65–123.
26. Hay OP. Second bibliography and catalogue of the fossil Vertebrata of North America. 1929; Volume 1. Carnegie Institution, Washington (DC).
27. Jaekel O. Über die Organisation der Petalodonten. Z Dtsch Geol Ges. 1899; 51:258–298.
28. Woodward AS. On a new species of *Edestus* from the Upper Carboniferous of Yorkshire. Q J Geol Soc London, 1917; 72:1–6.
29. Itano WM. A tooth of *Edestus* from the early Pennsylvanian of Cheshire, UK. Proc Yorkshire Geol Soc. 2013; 59:187–194.
30. Miller S. The American Palaeozoic fossils: a catalogue of the genera and species, with names of authors, dates, places of publication, etc. 1877; Published by the author. Cincinnati.
31. Trautschold H. Ueber *Edestus protopirata* Trd. Zeitschrift der Deutschen Geologischen Gesellschaft, 1888; 40:750–753.
32. Newberry JS, Worthen AH. Descriptions of new species of vertebrates, mainly from the Sub-Carboniferous limestone and Coal Measures of Illinois. Geol Surv Illinois, 1866; 2:9–134.
33. Watson DMS. *Edestus pringlei* sp. nov. Summary of Progress of the Geological Survey of Great Britain and the Museum of Practical Geology for the Year 1929. 1930; Part II, p. 69–73.
34. Hitchcock E. Account of the discovery of the fossil jaw of an extinct family of sharks, from the Coal Formation. Proc Amer Assoc Adv Sci. 1856; 9:229–230.
35. Hay OP. On the nature of *Edestus* and related genera, with descriptions of one new genus and three new species. Proc US Nat Mus. 1909; 37:43–61.
36. Missuna A. Ueber eine neue *Edestus*-Art aus den Karbon-Ablagerungen der Umgebungen von Kolomna. Bull Soc Impér Natural Moscou. 1908; 21:529–535.
37. Newberry JS. The Paleozoic fishes of North America. Monogr US Geol Surv. 1889; 16:1–340.
38. Itano WM. An abraded tooth of *Edestus* (Chondrichthyes, Eugeneodontiformes): Evidence for a unique mode of predation. T Kansas Acad Sci. 2015; 118:1–9. <https://doi.org/10.1660/062.118.0101>

39. Itano WM. A tooth whorl of *Edestus heinrichi* (Chondrichthyes, Eugeneodontiformes) displaying progressive macrowear. *T Kansas Acad Sci.* 2018; 121:125–133. <https://doi.org/10.1660/062.121.0214>
40. Itano WM. Oriented microwear on a tooth of *Edestus minor* (Chondrichthyes, Eugeneodontiformes): implication for dental function. *Palaeontologia Electronica* 2019; 22.2.39. <https://doi.org/10.26879/831>
41. Ramsay JB, Wilga CD, Tapanila L, Pruitt J, Pradel A, Schlader R, et al. Eating with a saw for a saw: functional morphology of the jaws and tooth-whorl in *Helicoprion davisii*. *J Morphol.* 2015; 276:47–64. <https://doi.org/10.1002/jmor.20319> PMID: 25181366
42. Waters CN, Waters RA, Barclay WJ, Davies JR. A lithostratigraphical framework for the Carboniferous successions of southern Great Britain (Onshore). *Brit Geol Surv Res Report*, 2009; RR/09/01.
43. Wright N, Zahirovic S, Müller RD, Seton M. Towards community-driven paleogeographic reconstructions: integrating open-access paleogeographic and paleobiology data with plate tectonics. *Biogeosciences* 2013; 10:1529–1541; <https://doi.org/10.5194/bg-10-1529-2013>
44. Ross CA, Ross JRP. Late Paleozoic sea levels and depositional sequences. *Cushman Foundation for Foraminiferal Research, Special Publication* 1986; 24:137–149.